# Direct numerical simulation of turbulence–mean field interactions in a stably stratified fluid

By M. G A L M I C H E[1]†, O. T H U A L[1] AND P. B O N N E T O N[2]

[1]Institut de Mécanique des Fluides de Toulouse, Allée du Professeur Camille Soula,
31400 Toulouse, France
[2]Département de Géologie et d'Océanographie, UMR CNRS 5805, Université Bordeaux 1,
33405 Talence, France

Freely decaying turbulent flows in a stably stratified fluid are simulated with a pseudo-spectral numerical code solving the fully nonlinear Navier–Stokes equations under the Boussinesq approximation with periodic boundary conditions. The flow is decomposed into a turbulent field and a horizontal mean flow $\bar{u}(z,t)$ defined as the average of the horizontal velocity component in a horizontal plane at height $z$ and time $t$. Similarly, the density field is decomposed into a turbulent field and a (stable) mean density profile $\bar{\rho}(z,t)$ defined as the average of the density field in a horizontal plane at height $z$ and time $t$. Attention is paid to the effect of the turbulent velocity field on an initial $z$-periodic horizontal mean flow (Simulation A) or an initial $z$-periodic perturbation of the mean density profile (Simulation B). Both A and B are performed under conditions of moderate and strong stratification and are compared to the non-stratified simulations.

Simulation A shows that the turbulence–mean flow interaction is strongly affected by the buoyancy forces. In the absence of a stratification, the mean flow perturbation decays rapidly due to the turbulent diffusion of momentum. When a moderate stratification is applied, the mean flow perturbation decays much more slowly whereas it oscillates and grows with time when the stratification is strong. These results are interpreted by defining a time-dependent eddy viscosity. Whereas the eddy viscosity coefficient has positive values in the non-stratified simulation, it is affected by the buoyancy forces and decreases after a period of order $N^{-1}$ in the stratified simulations (where $N$ is the Brunt–Väisälä frequency associated with the background linear stratification). At large time, we find that the eddy viscosity remains roughly zero when the stratification is moderate, whereas it oscillates but remains persistently negative in the strongly stratified case, which causes the horizontal mean flow to accelerate.

In Simulation B, we find that a perturbation in the mean density profile oscillates on a timescale of order $N^{-1}$ (where $N$ is the Brunt–Väisälä frequency associated with the background linear stratification) and remains almost unaffected by the turbulent field for large time. This shows that the stable stratification strongly inhibits the mixing efficiency of turbulence which usually tends to diffuse any scalar in non-stratified flows. We define a time-dependent eddy diffusivity coefficient which is found to take negative values after a period of order $N^{-1}$. For large times, the eddy diffusivity oscillates and its time-averaged value over a few turnover timescales is positive but

† Author to whom correspondence should be addressed, present address: LEGI, BP53 38041 Grenoble Cedex 9, France; galmiche@hmg.inpg.fr

small when the stratification is moderate, and roughly zero when the stratification is strong.

We conclude that the presence of a stable stratification strongly affects the temporal behaviour of the mean quantities $\bar{u}$ and $\bar{\rho}$ in turbulent flows and partly explains the formation of horizontal layers in stratified geofluids such as oceans and atmospheres.

## 1. Introduction

Oceans and atmospheres are usually stably stratified in density due to salinity and temperature vertical gradients. The dynamics of stratified geofluids are known to exhibit a very particular phenomenology and have been the subject of many experimental, numerical and theoretical studies. The issue of mass and momentum transport in stably stratified turbulent flows not only is interesting from a fundamental point of view but is also a key to better understanding the mixing and dynamical processes in environmental or industrial problems.

To investigate the effect of a stable density gradient on turbulent flows, the toy problem of *freely decaying turbulence* has already been extensively studied in laboratory experiments (see for instance the grid-turbulence experiments in salted water of Komori *et al.* 1983 and Itsweire, Helland & Van Atta 1986, and the wind tunnel experiments of Lienhard & Van Atta 1990 and Yoon & Warhaft 1990) and numerical simulations (Riley, Metcalfe & Weissman; Métais & Herring 1989; Gerz & Schumann 1991; Kimura & Herring 1996; Galmiche, Thual & Bonneton 1998). In such flows, complexity arises from the coexistence of two timescales: the turnover timescale associated with the eddy structures and the Brunt–Väisälä, or buoyancy period, associated with the buoyancy restoring forces acting on the fluid particles. Thanks to laboratory experiments and numerical simulations, it is now well known that the major effect of the buoyancy forces is to reduce dramatically the vertical kinetic energy and vertical turbulent transport, leading to the formation of vortical patches separated by strong horizontal vortex sheets. The first clear experimental evidence of this phenomenum has been given by Fincham, Maxworthy & Spedding (1996), whose results also show that the dissipation in the stratified turbulent flow is mainly controlled by the local horizontal vorticity.

When initially isotropic turbulence is subjected to a sufficiently strong stratification, one striking phenomenon is the oscillation in time of the buoyancy turbulent vertical flux between positive and negative (i.e. counter-gradient) values (Riley *et al.* 1981; Gerz & Schumann 1991). The development of counter-gradient fluxes in stratified flows is consistent with the general conclusions of the stability analysis and, using the framework of the rapid distortion theory, Hanazaki & Hunt (1996) have shown that the time-oscillation of the fluxes could be described well by a linear model. A detailed investigation of energy transfers in stratified turbulence is provided in Godeferd & Cambon (1994).

The effect of a uniform vertical mean shear on stratified decaying turbulence has been investigated experimentally by Piccirillo & Van Atta (1997) and numerically by Gerz, Schumann & Elghobashi (1989), Holt, Koseff & Ferziger (1992) and Jacobitz, Sarkar & Van Atta (1997) for instance. In the most strongly stratified flows, it was found that the vertical buoyancy flux not only oscillates as time evolves, but also remains persistently counter-gradient for large times. Persistent counter-gradient momentum fluxes have also been measured.

In the present paper we use direct numerical simulation to study freely decaying

stratified turbulence in the presence of a non-uniform vertical mean shear or a non-uniform stratification. The mean flow profile $\bar{u}$ and the mean density profile $\bar{\rho}$ are allowed to vary with height $z$ and time $t$ and we focus our attention on the signature of the initial turbulent velocity field on these profiles. There are many reasons to motivate these numerical experiments. First, we wish to get closer to realistic situations encountered in oceans and atmospheres which are generally subject to non-uniform stratification and stresses. Furthermore, these vertical variations modify the problem of turbulence–mean interaction considerably since the vertical dependence of the mean quantities is expected to induce vertical-dependent turbulent fluxes of buoyancy and momentum which may in turn affect the mean density and mean flow profiles. Thus, the time-dependence of the mean stratification and mean flow are strongly coupled with their vertical dependence. This crucial aspect of turbulence–mean interaction in stably stratified fluids has already been pointed out by Phillips (1972) and Posmentier (1977) and is a key point in explaining the formation of horizontal layers as observed in a number of laboratory experiments (e.g. Pearson & Linden 1983; Park, Whitehead & Gnanadeskian 1994) in the final stage of decay of turbulence.

The case where the fluctuation field has small amplitude compared to the variations in the mean fields has been extensively addressed using a linear stability analysis (e.g. Miles 1961; Howard 1961 and more recently Majda & Shefter 1998). In this paper the turbulence–mean field interaction is simulated in the more realistic situation where the amplitude of the variations in the mean fields is of the same order as the amplitude of the turbulent field. To describe this turbulence–mean interaction in the first stage of decay of turbulence, direct numerical simulation is a powerful tool which allows us to describe accurately the short-time evolution of the stratification and mean flow profiles.

We use a pseudo-spectral code to simulate the Navier–Stokes equations under the Boussinesq approximations. The computation domain is cubic, the boundary conditions are periodic in all directions (with periodicity $L$) and the initial turbulent velocity field is homogeneous and isotropic. When necessary, the results are ensemble-averaged over a set of realizations. The equations of motion and other theoretical considerations are provided in §2. The numerical methodology and the generation of the initial *turbulent* velocity field is described in §3.

We first study the effect of the turbulent field on a shear flow profile $\bar{u}(z)$ with uniform stratification $N$ (§4). The decay of turbulence is simulated in the presence of an initially imposed mean flow profile varying as $\cos(2\pi z/L)$. The simulations are performed under conditions of either moderate or strong stratification and are compared to the non-stratified case.

The effect of the turbulent field on a mean density profile is investigated in §5. The stable, background linear profile is initially perturbed by a periodic profile varying as $\cos(2\pi z/L)$ with no imposed mean shear. The simulations are performed under conditions of either moderate or strong stratification. The results from these numerical simulations are further discussed in §6. A summary and some concluding remarks are provided in §7.

## 2. Theoretical background

### 2.1. *Equations of motion*

We make the Boussinesq approximation, neglecting the density fluctuations except in the buoyancy term. We use a Cartesian coordinate system $(e_1, e_2, e_3)$ with the

| | Linear mean profile | $z$-Periodic mean profile | Fluctuations |
|---|---|---|---|
| $\boldsymbol{u}(\boldsymbol{x},t)$ | 0 | $\bar{\boldsymbol{u}}(z,t)$ | $\boldsymbol{u}_{pol}(\boldsymbol{x},t) + \boldsymbol{u}_{tor}(\boldsymbol{x},t)$ |
| $E_{kin}(t)$ | | $E_{\bar{u}}(t) + E_{\bar{v}}(t)$ | $E_{pol}(t) + E_{tor}(t)$ |
| $\rho(\boldsymbol{x},t)$ | $\bar{\rho}_l(z)$ | $\bar{\rho}_p(z,t)$ | $\rho'(\boldsymbol{x},t)$ |
| | | $\tilde{\rho}(\boldsymbol{x},t) = \bar{\rho}_p(z,t) + \rho'(\boldsymbol{x},t)$ | |
| $E_{pot}(t)$ | Reference state | $E_{\bar{\rho}}(t)$ | $E_{\rho'}(t)$ |

TABLE 1. Summary of the decomposition of the velocity and density fields. The velocity field is the sum of the $z$-periodic mean profile $\bar{\boldsymbol{u}}(z,t)$ and of the turbulent fluctuations. The turbulent fluctuations are the sum of the poloidal and toroidal velocity fields $\boldsymbol{u}_{pol}(\boldsymbol{x},t)$ and $\boldsymbol{u}_{pol}(\boldsymbol{x},t)$. The density field is the sum of the stable, linear mean profile $\bar{\rho}_l(z)$ (reference state with zero potential energy), the $z$-periodic mean profile $\bar{\rho}_p(z,t)$ and the turbulent fluctuations $\rho'(\boldsymbol{x},t)$. The density fluctuations from the linear mean profile are denoted by $\tilde{\rho}(\boldsymbol{x},t)$.
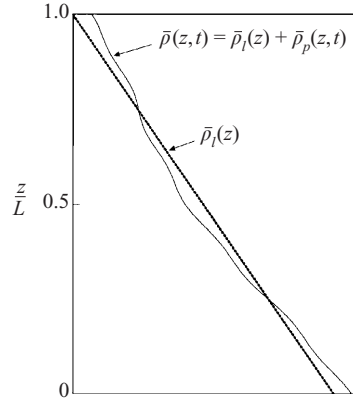


FIGURE 1. Sketch of the mean density profile decomposition. The mean density profile $\bar{\rho}(z,t)$ at time $t$ is the sum of the background linear profile $\bar{\rho}_l(z)$ and the periodic profile $\bar{\rho}_p(z,t)$.

$e_3$-direction antiparallel to the gravitational acceleration $\boldsymbol{g}$. The spatial coordinates are denoted by $(x,y,z) = \boldsymbol{x}$ and time by $t$. The velocity field is $\boldsymbol{u}(\boldsymbol{x},t) = (u,v,w)$ and the fluid density $\rho(\boldsymbol{x},t)$ may be decomposed as

$$\rho(\boldsymbol{x},t) = \bar{\rho}(z,t) + \rho'(\boldsymbol{x},t), \tag{2.1}$$

where $\bar{\rho}(z,t)$ is the spatial average of $\rho$ at time $t$ in the horizontal plane of height $z$ and $\rho'(\boldsymbol{x},t)$ is the density deviation from $\bar{\rho}$.

In this paper, fully periodic boundary conditions are used with periodicity $L$ for both the velocity and density fields. Then, $\bar{\rho}(z,t)$ is given by

$$\bar{\rho}(z,t) = \langle \rho(\boldsymbol{x},t) \rangle^{xy}, \tag{2.2}$$

where operator $\langle . \rangle^{xy}$ is defined by

$$\langle . \rangle^{xy} = \frac{1}{L^2} \int_0^L \int_0^L \cdot \, \mathrm{d}x \, \mathrm{d}y. \tag{2.3}$$

The mean density profile itself may be decomposed into a linear component $\bar{\rho}_l$ (the constant, background profile) and a $z$-periodic component $\bar{\rho}_p$ which allows for the non-uniformity of the stratification (see figure 1 and table 1):

$$\bar{\rho}(z,t) = \bar{\rho}_l(z) + \bar{\rho}_p(z,t). \tag{2.4}$$

Provided that at each level $\partial_z \bar{\rho} < 0$, the stratification is stable everywhere and the local Brunt–Väisälä frequency $\mathcal{N}$ is defined by

$$\mathcal{N}^2(z,t) = N^2 - \frac{g}{\rho_r}\frac{\partial \bar{\rho}_p(z,t)}{\partial z}. \tag{2.5}$$

Here, $g$ is the norm of $\boldsymbol{g}$, $\rho_r$ is a suitable reference density and

$$N^2 = -\frac{g}{\rho_r}\frac{\mathrm{d}\bar{\rho}_l(z)}{\mathrm{d}z} \tag{2.6}$$

is the squared Brunt–Väisälä frequency associated with the background linear stratification.

The density fluctuations from the background linear profile will be denoted by $\tilde{\rho}(\boldsymbol{x},t) = \rho(\boldsymbol{x},t) - \bar{\rho}_l(z) = \bar{\rho}_p(z,t) + \rho'(\boldsymbol{x},t)$. Then, the equations of motion under the Boussinesq approximation may be written as

$$\left.\begin{aligned} \nabla \cdot \boldsymbol{u} &= 0, \\ \partial_t \boldsymbol{u} + (\boldsymbol{u} \cdot \nabla)\boldsymbol{u} &= -\rho_r^{-1}\nabla p - g(\tilde{\rho}/\rho_r)\boldsymbol{e}_3 + \nu\nabla^2\boldsymbol{u}, \\ \partial_t \tilde{\rho} + (\boldsymbol{u} \cdot \nabla)\tilde{\rho} &= (\rho_r/g)N^2 w + \kappa\nabla^2\tilde{\rho}, \end{aligned}\right\} \tag{2.7}$$

where $\nabla = (\partial_x, \partial_y, \partial_z)$, $p$ is the pressure deviation from the hydrostatic profile, $\nu$ is the kinematic viscosity and $\kappa$ is the thermal diffusivity of the fluid.

### 2.2. *Decomposition of the flow field*

One can show (see Thual 1992) that an alternative description of any solenoidal velocity field $\boldsymbol{u} = (u,v,w)$ with periodic boundary conditions is provided by knowing:

(i) $w(\boldsymbol{x},t)$, the vertical velocity;

(ii) $\partial_x v - \partial_y u = \zeta(\boldsymbol{x},t)$, the vertical vorticity; and

(iii) $\bar{\boldsymbol{u}}(z,t) = \bar{u}(z,t)\boldsymbol{e}_1 + \bar{v}(z,t)\boldsymbol{e}_2$, the horizontal mean flow.

Here, the horizontal mean flow is defined by

$$\bar{\boldsymbol{u}}(z,t) = \langle \boldsymbol{u}(\boldsymbol{x},t)\rangle^{xy}, \tag{2.8}$$

where $\langle . \rangle^{xy}$ is defined by (2.3). In this decomposition, knowing the horizontal mean flow $\bar{\boldsymbol{u}}$ is crucial to reconstruct the complete velocity field $(u,v,w)$.

As in the present study fully periodic boundary conditions are used, the mean flow profile is also $z$-periodic and there is no uniform background shear.

Using the above $w$–$\zeta$–$\bar{\boldsymbol{u}}$ decomposition, the equations of motion become

$$\left.\begin{aligned} \nabla \cdot \boldsymbol{u} &= 0, \\ \partial_t \nabla^2 w - \nabla\wedge(\nabla\wedge[(\boldsymbol{u} \cdot \nabla)\boldsymbol{u}]) \cdot \boldsymbol{e}_3 &= -(g/\rho_r)\nabla_H^2\tilde{\rho} + \nu\nabla^4 w, \\ \partial_t \zeta + \nabla\wedge[(\boldsymbol{u} \cdot \nabla)\boldsymbol{u}] \cdot \boldsymbol{e}_3 &= \nu\nabla^2\zeta, \\ \partial_t\bar{u} + \partial_z\langle uw\rangle^{xy} = \nu\partial_{zz}\bar{u}, \quad \partial_t\bar{v} &+ \partial_z\langle vw\rangle^{xy} = \nu\partial_{zz}\bar{v}, \\ \partial_t\tilde{\rho} + (\boldsymbol{u} \cdot \nabla)\tilde{\rho} &= (\rho_r/g)N^2 w + \kappa\nabla^2\tilde{\rho}, \end{aligned}\right\} \tag{2.9}$$

where $\nabla_H = (\partial_x, \partial_y, 0)$.

It is useful to make the connection between the $w$–$\zeta$–$\bar{\boldsymbol{u}}$ decomposition and the often-used poloidal–toroidal decomposition (see for instance Riley & Lelong 2000):

$$\boldsymbol{u}(\boldsymbol{x},t) = \bar{\boldsymbol{u}}(z,t) + \boldsymbol{u}_{pol}(\boldsymbol{x},t) + \boldsymbol{u}_{tor}(\boldsymbol{x},t). \tag{2.10}$$

Here the poloidal and toroidal velocities are defined by

$$\boldsymbol{u}_{pol}(\boldsymbol{x},t) = \nabla\wedge[\nabla\wedge E(\boldsymbol{x},t)\boldsymbol{e}_3] \quad \text{and} \quad \boldsymbol{u}_{tor}(\boldsymbol{x},t) = \nabla\wedge[B(\boldsymbol{x},t)\boldsymbol{e}_3], \tag{2.11}$$

where functions $E$ and $B$ are such that $w = -\nabla_H^2 E$ and $\zeta = -\nabla_H^2 B$. The poloidal component $\boldsymbol{u}_{pol}$ has zero vertical vorticity and the toroidal component $\boldsymbol{u}_{tor}$ has zero vertical velocity. In this decomposition, the horizontal mean flow field $\bar{\boldsymbol{u}}$ cannot be included either in the poloidal or in the toroidal fields and is again necessary to reconstruct the complete velocity field $(u, v, w)$. In the limit of small Froude numbers (defined below), e.g. in the final stage of decay of turbulence, the poloidal and toroidal energies may be associated with the wavy and vortical motions respectively (see Riley *et al.* 1981; Riley & Lelong 2000 and also Staquet & Riley 1989 for the isopycnal version of the decomposition).

### 2.3. *Energy partition*

As the computation domain is periodic, the kinetic energy per unit mass averaged over the box may be written as

$$E_{kin}(t) = E_{\bar{u}}(t) + E_{\bar{v}}(t) + E_{pol}(t) + E_{tor}(t), \tag{2.12}$$

where $E_{\bar{u}}(t) = (1/2)\langle\bar{u}^2\rangle^z$ (respectively $E_{\bar{v}}(t) = (1/2)\langle\bar{v}^2\rangle^z$) is the energy of the $x$-component (respectively the $y$-component) of the mean flow, $E_{pol}(t) = (1/2)\langle\boldsymbol{u}_{pol}^2\rangle^{xyz}$ is the poloidal energy and $E_{tor}(t) = (1/2)\langle\boldsymbol{u}_{tor}^2\rangle^{xyz}$ is the toroidal energy. Here,

$$\langle.\rangle^z = \frac{1}{L}\int_0^L . \, \mathrm{d}z \quad \text{and} \quad \langle.\rangle^{xyz} = \frac{1}{L^3}\int_0^L\int_0^L\int_0^L . \, \mathrm{d}x\,\mathrm{d}y\,\mathrm{d}z. \tag{2.13}$$

Taking the linear stratification $\bar{\rho}_l$ as the reference state, the potential energy may be written as

$$E_{pot}(t) = E_{\bar{\rho}}(t) + E_{\rho'}(t), \tag{2.14}$$

where $E_{\bar{\rho}}(t) = (1/2)(g/\rho_r N)^2\langle\bar{\rho}_p^2\rangle^z$ is the energy of the density periodic mean profile and $E_{\rho'}(t) = (1/2)(g/\rho_r N)^2\langle\rho'^2\rangle^{xyz}$ is the *turbulent* potential energy, (Note that $E_{\bar{\rho}}$ may also be called the *background* potential energy, and only $E_{\rho'}$ makes up part of the *available* energy.)

The total† energy $E(t)$ in the box at time $t$ is then

$$E(t) = E_{kin}(t) + E_{pot}(t). \tag{2.15}$$

The velocity, density and energy decompositions are summarized in table 1.

### 2.4. *Context of the problem*

In models of stratified geophysical flows such as oceanic or atmospheric flows, one of the main difficulties is generally to model the effect of turbulence on the mean quantities $\bar{\boldsymbol{u}}$ and $\bar{\rho}$, especially when the energy is transferred from small to large scales. The present analysis does not aim to take into account the effects of specific boundary conditions or external forcing encountered in realistic situations, but is intended to discuss the turbulence-mean interaction from a general point of view. Taking the average in a horizontal plane of the equation of $\tilde{\rho}$, we obtain the evolution equation for $\bar{\rho}(z,t)$ as

$$\partial_t\bar{\rho} = -\partial_z F_\rho + \kappa\partial_{zz}\bar{\rho}, \tag{2.16}$$

---

† Here the word 'total' has to be understood in the mechanical sense ('kinetic plus potential'), not the thermodynamical sense.

where $F_\rho = \langle \rho w \rangle^{xy}$ is the vertical turbulent buoyancy flux. Similarly, the equation for $\bar{u}(z,t)$ is

$$\partial_t \bar{u} = -\partial_z F_u + v \partial_{zz} \bar{u}, \qquad (2.17)$$

where $F_u = \langle uw \rangle^{xy}$ is the vertical turbulent momentum flux and a third equation for $\bar{v}(z,t)$ is obtained with $F_v = \langle vw \rangle^{xy}$. In the absence of a stratification (i.e. when $\rho$ is a passive scalar), the eddy fluxes of mass and momentum are generally modelled using the concept of eddy diffusivity and viscosity which depend on local properties such as the mixing length and intensity of turbulence. In most cases, these eddy coefficients have positive values. When a stable stratification is present, the buoyancy term does not appear explicitly in (2.16) and (2.17), but the stratification affects the fluctuations of the flow field and thus the turbulent fluxes in a way that is still poorly understood. The mechanisms affecting the transport of mass and momentum in a stratified fluid are partly due to the wavy properties of the medium which make allowance for the propagation, distortion and interactions of internal gravity waves. This has an effect on the correlations $\langle uw \rangle^{xy}$ and $\langle \rho w \rangle^{xy}$ and significantly modifies the concepts of eddy viscosity and diffusivity. For instance, Galmiche, Thual & Bonneton (2000) have shown with direct numerical simulation that the interaction of two internal waves can produce strong horizontal mean currents, which, of course, cannot be reproduced by classical eddy viscosity models.

A number of numerical simulations (Riley *et al.* 1981; Gerz *et al.* 1989) and results from the rapid distortion theory (Hanazaki & Hunt 1996) show that in decaying, stratified turbulent flows with homogeneous and isotropic initial conditions, the buoyancy fluxes tend to oscillate and eventually become counter-gradient. When a vertical mean shear is present, the direct numerical simulations of Gerz *et al.* (1989) show that the buoyancy and momentum turbulent fluxes both oscillate and eventually become counter-gradient. However, when the mean shear and stratification are both uniform, the fluxes do not depend on height $z$† and it is clear from (2.16) and (2.17) that the mean profiles $\bar{\rho}$ and $\bar{u}$ remain unaffected as the turbulence evolves (note that in this case the average operator $\langle . \rangle^{xy}$ may be replaced by a statistical operator under assumptions of ergodicity). Nevertheless, Phillips (1972) and Posmentier (1977) have shown, with physical arguments, that for a sufficiently large stratification, an initial perturbation in the mean density profile may grow under the effect of the counter-gradient buoyancy fluxes, leading to the formation of horizontal layers. Similarly, one may expect that shear layers can develop under the effect of the counter-gradient momentum fluxes when the turbulent field is perturbed by a non-uniform mean shear profile. One consequence of these phenomena is that the concepts of positive eddy viscosity and diffusivity fail and may be replaced by negative coefficients. This is the key point of the present study.

## 3. Numerical methodology

In this section the numerical method used to solve equations (2.9) is described, as well as the generation of the *turbulent* part of the initial conditions prescribed in the subsequent simulations.

The flow evolves with no external forcing in a cubic box of size $L$. The equations of motion (2.9) are solved for variables $w$, $\zeta$, $\bar{u}$ and $\tilde{\rho}$ using a pseudo-spectral code (see Thual 1992) with fully periodic boundary conditions and $64^3$ grid points. Some

---

† This supposes that, as argued by Townsend (1976), the momentum and buoyancy fluxes only depend on the local mean gradients.

validation runs have been performed with $128^3$ grid points (the choice of the resolution is discussed in §3.2). All the variables are Fourier-transformed and the equations are solved in the Fourier space, except when computing the nonlinear terms, which are calculated in the physical space. A second-order, *slaved-frog* temporal scheme (see Frisch, She & Thual 1986) is used.

### 3.1. *First step*

The first step is to compute a non-divergent, random velocity field following Gaussian statistics with homogeneity and isotropy properties. Following Orszag & Patterson (1972), we prescribe the energy spectrum:

$$\frac{\mathcal{E}(k,0)}{E_{kin}(0)} = \frac{32}{3k_I}\sqrt{\frac{2}{\pi}}\left(\frac{k}{k_I}\right)^4 \exp(-2(k/k_I)^2), \tag{3.1}$$

where $\mathcal{E}(k,0)$ is the initial energy associated with wavenumber $k$, $E_{kin}(0) = E_{pol}(0) + E_{tor}(0)$ is the energy of the initial, Gaussian velocity field and $k_I$ is the injection wavenumber (taken equal to $4.76 \times 2\pi/L$). We define an integral lengthscale $l(t)$ by

$$l(t) = \frac{3\pi}{4}\frac{\displaystyle\int_0^\infty (\mathcal{E}(k,t)/k)\mathrm{d}k}{\displaystyle\int_0^\infty \mathcal{E}(k,t)\mathrm{d}k} \tag{3.2}$$

and the root-mean-square velocity $u_{rms}(t)$ by $E_{kin}(t) = (3/2)u_{rms}^2(t)$.

### 3.2. *Second step, validation and strategy*

From this Gaussian initial condition, a short precomputation is performed with no stratification and no mean shear imposed in order to obtain a non-Gaussian velocity field where nonlinear transfers are developed.

This simulation is stopped at $t_0 = 0.84l(0)/u_{rms}(0)$. Then, the value of the velocity-derivative skewness

$$S = -\langle(\partial_x u)^3\rangle^{xyz}/[\langle(\partial_x u)^2\rangle^{xyz}]^{3/2} \tag{3.3}$$

is of order 0.5 (see figure 2), which is typical of well-developed nonlinear transfers (see for instance the experimental results of Mills *et al.* 1958). The isotropic, homogeneous turbulent field obtained is denoted by $\boldsymbol{u}_{iht}(\boldsymbol{x})$ and is used to initialize the subsequent numerical experiments ($t = t_0$).

Using, for convenience, the notation $u_0' = u_{rms}(t_0)$ and $l_0 = l(t_0)$, this velocity field has a Reynolds number $Re = u_0'l_0/\nu = 55$ with $l_0$ of order one twelfth of $L$ (this corresponds to $R_\lambda = u_0'\lambda/\nu \simeq 41$ where $\lambda$ is the Taylor microscale). The velocity field in a vertical cross-section at $t = t_0$ is shown on figure 3.

Due to isotropy, the velocity field $\boldsymbol{u}_{iht}(\boldsymbol{x})$ satisfies $E_{pol}(t_0) \simeq E_{tor}(t_0)$, a small discrepancy being due to the random choice of the Gaussian field at $t = 0$. For the same reason, a non-zero mean flow is necessarily present at $t = t_0$ but the amount of energy associated with this mean flow is only a small part of the total kinetic energy ($E_{\bar{u}}(t_0) \simeq E_{\bar{v}}(t_0) \simeq 3 \times 10^{-3}E_{kin}(t_0)$).

We have performed a preliminary simulation for validation, with no stratification and no imposed mean flow in order to check that the numerical code correctly reproduces the decay of homogeneous, isotropic turbulence. In this simulation, the integral lengthscale of the turbulent field increases slowly (not shown) but does not exceed $L/7$ to $L/6$ after a few turnover timescales, which ensures that the simulation is not box-limited in the time period considered.
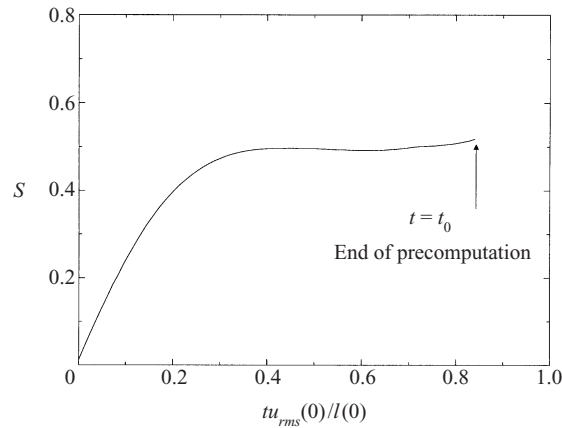
FIGURE 2. Evolution of the velocity-derivative skewness coefficient $S(t)$ in the precomputation. The time unit is the initial turnover timescale of turbulence $l(0)/u_{rms}(0)$. At $t = 0$, the velocity field has Gaussian statistics and thus $S(0) \simeq 0$. The precomputation is stopped when the nonlinear transfers are sufficiently developed ($t = t_0 \simeq 0.84l(0)/u_{rms}(0)$). Then, $S(t_0) \simeq 0.5$ and the velocity field obtained is used as the initial turbulent velocity field for the numerical experiments.
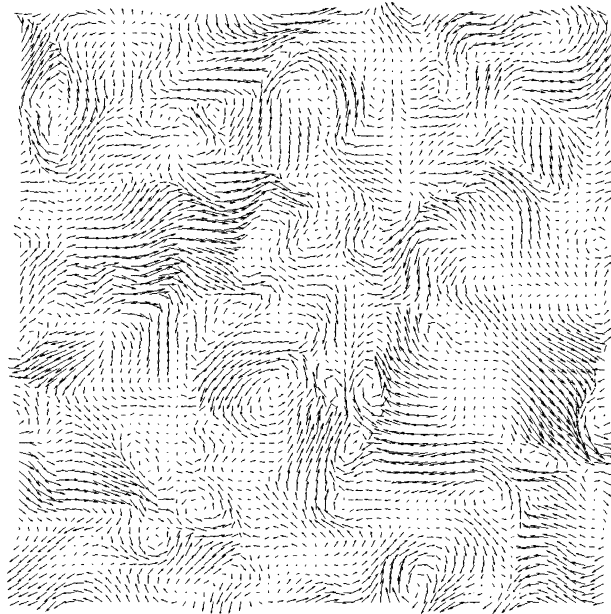


FIGURE 3. Cross-section of the velocity field $u_{iht}(x)$ (end of the precomputation and beginning of the simulations).

The decay of the kinetic energy in the computation domain tends to the power law $(t - t_0)^{-p}$ with $p \simeq 1.5$ (see figure 4). This value is close to the theoretical value 1.43 derived by Lesieur & Schertzer (1978) for low-Reynolds-number turbulence (this value was derived in the case of an energy spectrum varying as $k^4$ at low wavenumbers and with auto-similarity assumptions), but is slightly higher than the value measured in laboratory experiments on grid turbulence (e.g. Corrsin 1951).

The numerical experiments do not involve as many scales as laboratory experiments at high Reynolds number, due to low resolution. However, the decay of the turbulent
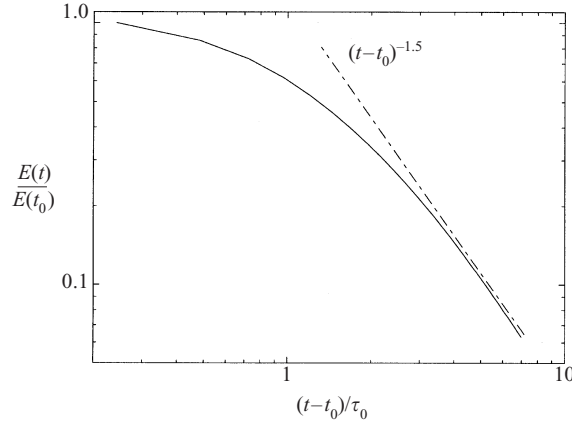
FIGURE 4. Decay of the total kinetic energy $E(t)$ in the preliminary simulation of turbulence with no stratification and no imposed mean flow initially. The time unit is $\tau_0 = l_0/u_0'$, the turnover timescale of turbulence at $t = t_0$. After a few turnover timescales, $E(t)$ decreases as $(t - t_0)^{-1.5}$.

kinetic energy and the development of nonlinear transfers are well reproduced in the validation run, which allows for qualitative interpretation of the global energetic properties of the simulated flows. These low-resolution simulations also provide a good starting point for theoretical analysis and comparison with models (Galmiche & Hunt 2002).

The results presented in this paper were not significantly changed when using $128^3$ grid points (with the same injection lengthscale, wavenumber range multiplied by two and Reynolds number of order 110). In some cases, however, the flow was found to be rather sensitive to the initial conditions. Thus, several realizations of each experiment have been performed and, when necessary, ensemble averages have been computed over the set of realizations. To do so, the resolution has to be chosen such that the computation time for each run is not excessive. Thus, all the simulations were performed using $64^3$ grid points. The difference between the realizations is the Gaussian sample used at the beginning of each precomputation, but the same energy spectrum (3.1) is prescribed at $t = 0$ in all cases and the velocity field has the same spectral and energetic properties at $t = t_0$.

## 4. Effect of turbulence on a stratified shear flow profile

### 4.1. *Definition of the simulations*

We first simulate the evolution of the horizontal mean flow profile $\bar{u}(z, t)$ under the effect of the decaying turbulence when the initial velocity field is affected by a specified mean profile $\bar{u}(z, t_0)$ (associated with the non-uniform vertical mean shear profile $d\bar{u}(z, t_0)/dz$). The isotropic, homogeneous turbulent field $\boldsymbol{u}_{iht}(\boldsymbol{x})$ generated as described in §3 is used as the *turbulent* part of the initial velocity field. The initial stratification is here uniform (i.e. $\bar{\rho}_p(z, t_0) = 0$) and only the case of zero initial density perturbations is considered (i.e. $E_{\rho'}(t_0) = 0$). Some details on the effect of initial density perturbations on decaying turbulence may be found in the numerical simulations of Métais & Herring (1989) and in the linear analysis of stratified turbulent shear flows by Hanazaki & Hunt (1996) and Galmiche & Hunt (2002).

The initial velocity field is affected by the horizontal mean flow in the fundamental

| Run | $\dfrac{E_{\bar{u}}(t_0)}{E(t_0)}$ | $\dfrac{E_{\bar{v}}(t_0)}{E(t_0)}$ | $\dfrac{E_{pol}(t_0)}{E(t_0)}$ | $\dfrac{E_{tor}(t_0)}{E(t_0)}$ | $\dfrac{E_{\bar{p}}(t_0)}{E(t_0)}$ | $\dfrac{E_{\rho'}(t_0)}{E(t_0)}$ | $Re(t_0)$ | $Fr(t_0)$ | $Pr$ | $n_r$ |
|-----|------|------|------|------|------|------|------|------|------|------|
| ANS | $\simeq \frac{1}{3}$ | $\simeq 0$ | $\simeq \frac{1}{3}$ | $\simeq \frac{1}{3}$ | 0 | 0 | 55 | $\infty$ | 1 | 6 |
| AMS | $\simeq \frac{1}{3}$ | $\simeq 0$ | $\simeq \frac{1}{3}$ | $\simeq \frac{1}{3}$ | 0 | 0 | 55 | 1.2 | 1 | 6 |
| ASS | $\simeq \frac{1}{3}$ | $\simeq 0$ | $\simeq \frac{1}{3}$ | $\simeq \frac{1}{3}$ | 0 | 0 | 55 | 0.12 | 1 | 6 |
| BNS | $\simeq 0$ | $\simeq 0$ | $\simeq \frac{1}{3}$ | $\simeq \frac{1}{3}$ | $\simeq \frac{1}{3}$ | 0 | 55 | $\infty$ | 1 | 1 |
| BMS | $\simeq 0$ | $\simeq 0$ | $\simeq \frac{1}{3}$ | $\simeq \frac{1}{3}$ | $\simeq \frac{1}{3}$ | 0 | 55 | 1.2 | 1 | 1 |
| BSS | $\simeq 0$ | $\simeq 0$ | $\simeq \frac{1}{3}$ | $\simeq \frac{1}{3}$ | $\simeq \frac{1}{3}$ | 0 | 55 | 0.12 | 1 | 1 |

TABLE 2. Definition of Simulations ANS, AMS, ASS, BNS, BMS and BSS. Letter A refers to the simulations of turbulence in the presence of an initial horizontal mean current; B refers to those in the presence of an initial perturbation of the mean density profile. Letters NS, MS and SS stand for non-stratified, moderately stratified and strongly stratified respectively. The number of realizations is denoted by $n_r$.

mode in the $x$-direction with amplitude $U_0$:

$$\boldsymbol{u}(\boldsymbol{x}, t_0) = \boldsymbol{u}_{iht}(\boldsymbol{x}) + U_0 \cos(2\pi z/L)\boldsymbol{e}_1. \tag{4.1}$$

The value of $U_0$ was chosen by considering the case of an equipartition between the initial poloidal, toroidal and mean flow energies:

$$E_{\bar{u}}(t_0) \simeq E_{pol}(t_0) \simeq E_{tor}(t_0) \simeq \tfrac{1}{3}E(t_0), \tag{4.2}$$

which requires $U_0/u_0' = \sqrt{3}$. As already mentioned in §3, the initial mean flow profile ($t = t_0$) is slightly affected by the small mean flow harmonics of $\boldsymbol{u}_{iht}$. The energy of these harmonics is only $\simeq 1\%$ of the energy of the imposed fundamental mode.

A suitable measure of the intensity of the stratification is given by the initial turbulent Froude number $Fr = u_0'/Nl_0$. Two values of $Fr$ are used: moderately stratified simulation (AMS), $Fr = 1.2$; strongly stratified simulation (ASS), $Fr = 0.12$. The Froude number may be written as $N^{-1}/\tau_0$, where $\tau_0 = l_0/u_0'$ is the initial turnover timescale. Thus, $Fr$ is the ratio of the buoyancy timescale to the initial turnover timescale of turbulence. For comparison, a non-stratified simulation (BNS) was performed ($Fr = \infty$), by ignoring the buoyancy terms in equations (2.9).

In all the simulations, the Prandtl number $P = \nu/\kappa$ is taken equal to unity. This value is far from the value known for salted water (of order 800) used in laboratory experiments. However, as pointed out by Métais & Herring (1989), this Prandtl number equal to unity may be seen as an effective eddy Prandtl number for the simulated large-scale structures.

Although the simulations are fully defined by the Froude, Reynolds and Prandtl numbers and the mean flow amplitude, it is useful to define, in the stratified simulations, a $z$-dependent, local Richardson number by $Ri(z) = (N/\partial_z \bar{u}(z))^2$, knowing that this definition fails where the mean flow velocity has an extremum. In Simulation AMS, $Ri(z)$ varies between 1 and infinity, whereas it varies between 100 and infinity in Simulation ASS. This indicates that the mean shear perturbation has small amplitude compared to the intensity of the stratification, particularly in Simulation ASS. In both cases, $Ri$ is everywhere higher than the critical value $Ri_c = 0.25$ provided by the linear stability analysis.

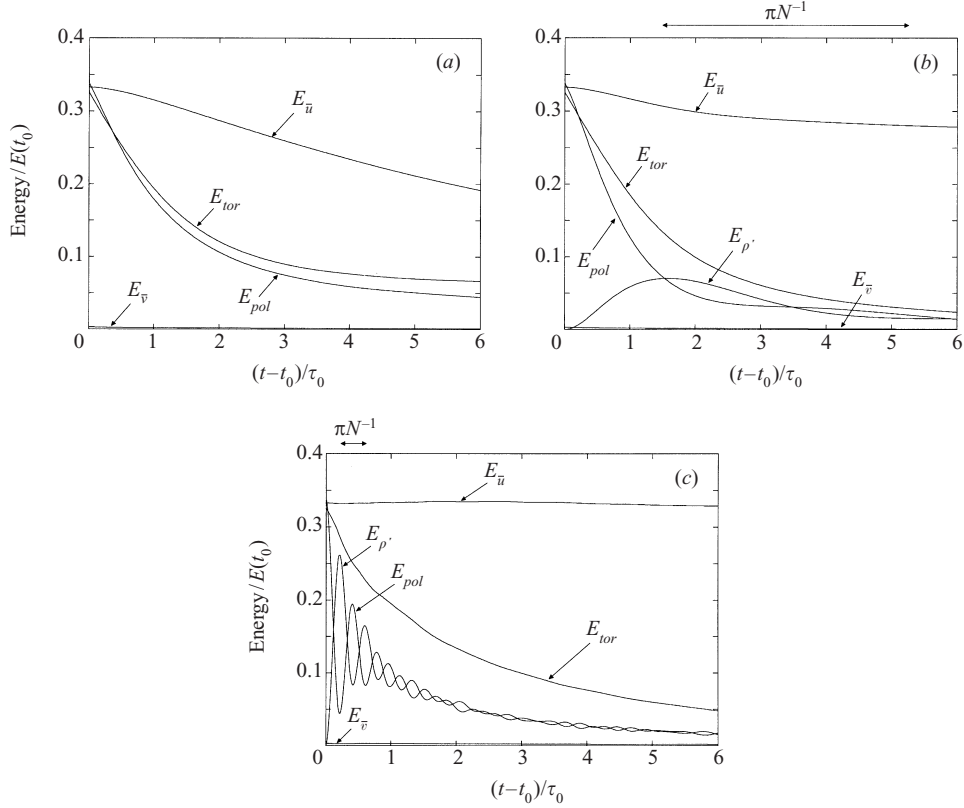The definition of the simulations is summarized in table 2.

FIGURE 5. Evolution of energies $E_{pol}$, $E_{tor}$, $E_{\bar{u}}$, $E_{\bar{v}}$ and $E_{\rho'}$ in Simulations (*a*) ANS, (*b*) AMS and (*c*) ASS (in Simulation ANS, $E_{\rho'}$ is not shown since the density fluctuations play no role in the flow dynamics). In these simulations, $E_{\bar{u}} \simeq E_{pol} \simeq E_{tor}$ and $E_{\rho'} = 0$ initially. The time unit is $\tau_0 = l_0/u'_0$, the turnover timescale of turbulence at $t = t_0$.

## 4.2. *Evolution of the turbulent and mean quantities*

The energies $E_{pol}$, $E_{tor}$, $E_{\bar{u}}$, $E_{\bar{v}}$ and $E_{\rho'}$ are plotted as a function of time on figure 5 for each simulation. On these plots, the time unit is $\tau_0 = l_0/u'_0$ and all the energies are normalized by the initial total energy $E(t_0)$.

In the non-stratified simulation (Simulation ANS), we observe a monotonic decay of the mean flow energy $E_{\bar{u}}$ as a result of the energy cascade to smaller scales of the flow. It is also observed that the toroidal energy decays more slowly than the poloidal energy. Although the mean shear distribution is non-uniform here, this result is consistent with the linear computations of Townsend (1976) which show that the vertical turbulent fluctuations decay faster than the horizontal fluctuations when an initially isotropic turbulent field is subject to a vertical mean shear.

In the stratified simulations (AMS and ASS), oscillating exchanges take place between the poloidal energy $E_{pol}$ and the potential energy $E_{\rho'}$. The oscillations are less intense and slower in the moderately stratified case than in the strongly stratified case. Their amplitude is damped after a few Brunt–Väisälä periods. These oscillations with a timescale of order $\pi N^{-1}$ have already been observed in previous numerical simulations of unsheared turbulence (e.g. Métais & Herring 1989) and successfully described in the framework of the rapid distortion theory by Hanazaki & Hunt (1996). At the end of the simulations, the poloidal and turbulent potential energies
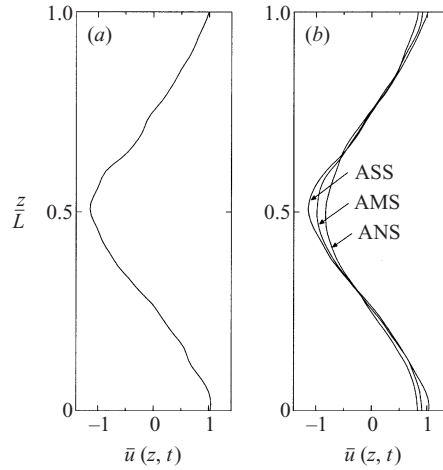
FIGURE 6. Mean flow profile $\bar{u}$ in Simulations ANS, AMS and ASS. Here the velocity scale is $U_0$, the amplitude of the perturbation imposed at $t = t_0$. (a) $t = t_0$ (the initial mean flow profile not only includes the fundamental imposed at $t = t_0$ but also the other modes present in the turbulent velocity field). (b) $t = t_0 + 4\tau_0$.

are roughly equipartitioned, whereas the toroidal energy $E_{tor}$ decays monotonically and more slowly. Then, the flow field may be seen as the superposition of the vortical field and a wave field with 'mean' energy $E_{pol} + E_{\rho'}$. After six turnover timescales, the ratio $(E_{pol} + E_{\rho'})/E_{tor}$ is 1.1 in the moderately stratified simulation AMS and 0.7 in the strongly stratified simulation ASS. It is interesting to note that the toroidal energy is dissipated faster in the moderately stratified case than in the strongly stratified case (after six turnover timescales we have $E_{tor} \simeq 0.025E(t_0)$ in Simulation AMS whereas we have $E_{tor} \simeq 0.05E(t_0)$ in Simulation ASS). It seems that in the strongly stratified case, the turbulent motions are rapidly converted into coherent vortical motions which are dissipated more slowly.

As the initial stratification is uniform in these simulations, the energy $E_{\bar{\rho}}$ starts from zero and is found to remain much lower than the other energies in the computation domain (not plotted). Similarly, the mean flow energy $E_{\bar{v}}$ in direction $e_2$ remains very low throughout the simulations.

Several realizations of these numerical experiments were performed but quantities $E_{pol}$, $E_{tor}$, $E_{\rho'}$, $E_{\bar{\rho}}$ and $E_{\bar{v}}$ are plotted only once, since they were found to evolve similarly in each realization.

We now focus our attention on the evolution of the mean flow energy $E_{\bar{u}}$. Whereas in the absence of a stratification (Simulation ANS) the mean flow is classically damped by the turbulent stresses, it is much more persistent when a stratification is applied (Simulations AMS and ASS).

After six turnover timescales, we have $E_{\bar{u}}/E_{\bar{u}}(t_0) \simeq 0.98$ in the strongly stratified simulation ASS, 0.85 in the moderately stratified simulation AMS, and 0.6 in the non-stratified simulation ANS. The mean flow profiles at time $(t - t_0) = 4\tau_0$ are shown on figure 6.

Unlike the other energies, the evolution of the mean flow energy $E_{\bar{u}}$ is found to be quite sensitive to the initial conditions although the global tendency is the same from one realization to another.

On figure 7(a), we have plotted the results for two realizations in the non-stratified, moderately stratified and strongly stratified cases. The mean flow $\bar{u}(z,t)$ may be
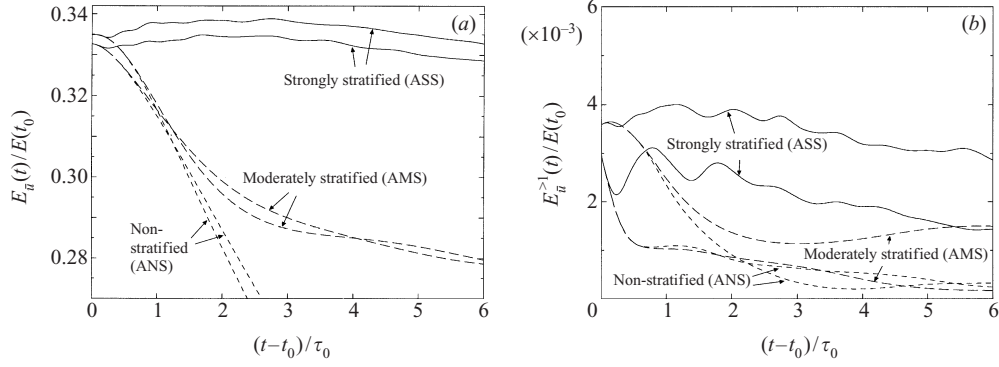
FIGURE 7. Evolution of ($a$) $E_{\bar{u}}$, the energy of the mean flow profile and ($b$) $E_{\bar{u}}^{>1}$, the energy of the harmonics with wavenumbers $> 2\pi/L$ in simulations ANS (dashed lines), AMS (long-dashed lines) and ASS (solid lines). The time unit is $\tau_0 = l_0/u_0'$, the turnover timescale of turbulence at $t = t_0$. For comparison, two realizations of each experiment have been plotted.
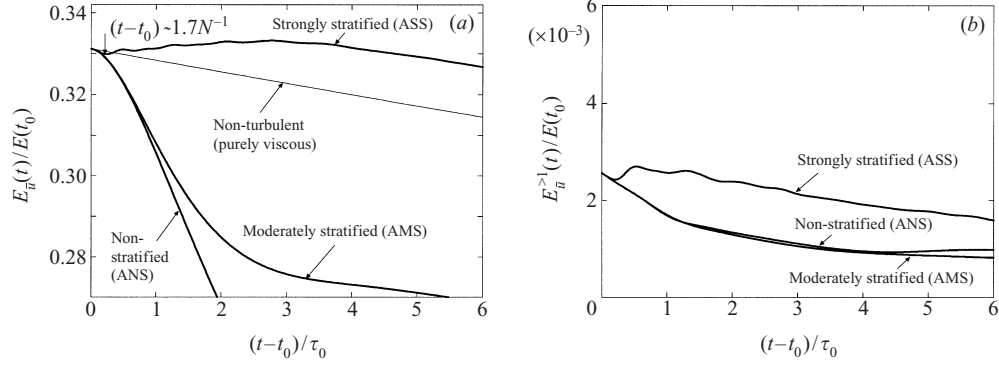


FIGURE 8. Ensemble-averaged evolution of ($a$) $E_{\bar{u}}$, the energy of the mean flow profile and ($b$) $E_{\bar{u}}^{>1}$, the energy of the harmonics with wavenumbers $> 2\pi/L$ in simulations ANS, AMS and ASS. The time unit is $\tau_0 = l_0/u_0'$, the turnover timescale of turbulence at $t = t_0$. Here, the ensemble averages have been performed over six realizations for each experiment. For comparison, the analytical solution for $E_{\bar{u}}(t)$ has been plotted when the effect of turbulence is ignored (purely viscous decay).

decomposed as

$$\bar{u}(z,t) = \bar{u}^1(z,t) + \bar{u}^{>1}(z,t), \tag{4.3}$$

where $\bar{u}^1$ is the fundamental (which corresponds to the scale of the mode $U_0 \cos(2\pi z/L)$ imposed at $t = t_0$), and $\bar{u}^{>1}$ is the sum of the harmonics with wavenumbers greater than $2\pi/L$. The mean flow energy is then

$$E_{\bar{u}}(t) = E_{\bar{u}}^1(t) + E_{\bar{u}}^{>1}(t), \tag{4.4}$$

where $E_{\bar{u}}^1 = (1/2)\langle(\bar{u}^1)^2\rangle^z$ and $E_{\bar{u}}^{>1} = (1/2)\langle(\bar{u}^{>1})^2\rangle^z$. The energy $E_{\bar{u}}^{>1}$ is plotted on figure 7($b$) for two realization of runs ANS, AMS and ASS.

In order to have a more general description of the mean flow evolution, ensemble averages have been performed over a set of six realizations. The number of realizations was chosen such that the averaged results were not significantly modified when using more realizations.

The results are shown on figure 8. We have also plotted the analytical solution for $E_{\bar{u}}$ obtained when the effect of the turbulence is ignored (this corresponds to the

purely viscous decay of the fundamental mean flow mode imposed at $t = t_0$). Note on figure 8($b$) that the quantity $E_{\bar{u}}^{>1}$ is almost unaffected by a moderate stratification since its evolution is similar in simulations AMS (moderately stratified) and ANS (non-stratified). Some weak oscillations of $E_{\bar{u}}^{>1}$ are observed in the strongly stratified simulation (ASS). However, $E_{\bar{u}}^{>1}$ remains much lower than $E_{\bar{u}}^1$ and $E_{\bar{u}} \simeq E_{\bar{u}}^1$ at any time in all three simulations. Thus, the energy plotted on figure 8($a$) is in fact mainly the energy of the fundamental mode.

When a moderate stratification is applied (Simulation AMS), the turbulent diffusion of momentum remains efficient during one or two turnover timescales and $E_{\bar{u}}$ decays as in the non-stratified, experiment (ANS). After two or three turnover timescales, the effect of the restoring buoyancy forces causes the fluid particles to reduce their vertical motion which affects the turbulent stresses and slows down the mean flow decay. After four or five turnover timescales, the turbulence becomes almost inefficient in affecting the mean flow and the rate of decay of $E_{\bar{u}}$ tends to the viscous rate.

In the strongly stratified simulation (ASS), the effect of the buoyancy forces on the mean flow is more dramatic. In the very early stages of decay, the evolution of $E_{\bar{u}}$ is close to the decay observed in the non-stratified simulation (ANS), but the mean flow is affected by the stratification as soon as $t - t_0 \simeq 0.2\tau_0$ ($\simeq 1.7N^{-1}$). At this time, $E_{\bar{u}}$ increases and not only starts oscillating but also continues increasing during two or three turnover timescales. $E_{\bar{u}}$ becomes greater than the viscous solution when $t - t_0 \simeq 0.35\tau_0$ ($\simeq 3N^{-1}$). After four turnover timescales, $E_{\bar{u}}$ decays at the viscous rate but remains larger than the viscous solution. These results show that the buoyancy forces cause the turbulent motions to transfer energy to the mean motion, which induces a net acceleration of the horizontal current.

### 4.3. *Eddy diffusion of momentum*

Following the discussion of §2.4 on turbulence–mean field interactions, the evolution of the horizontal mean flow may be interpreted in terms of eddy diffusion of momentum. As the fundamental mode $\bar{u}^1(z, t)$ of the mean flow profile largely dominates the other harmonics $\bar{u}^{>1}(z, t)$ throughout the simulations, we focus our attention on the equation for $\bar{u}^1(z, t)$:

$$\partial_t \bar{u}^1 + \partial_z [\langle uw \rangle^{xy}]^1 = \nu \partial_{zz} \bar{u}^1, \tag{4.5}$$

where $[\langle uw \rangle^{xy}]^1$ is the fundamental mode of the vertical profile of the momentum flux $\langle uw \rangle^{xy}$.

The profiles of the mean flow increment $\bar{u}^1(z, t) - \bar{u}^1(z, t_0)$ are plotted on figure 9 in one realization of Simulations ANS, AMS and ASS at different times. These plots show that the fundamental has almost constant spatial phase in the non-stratified and moderately stratified simulation. A vertical shift is observed in the strongly stratified simulations, which may be due to the global oscillations of the velocity field. However, this vertical shift remains small throughout the simulation. Thus, the mean flow mode may be seen as the solution of the following diffusion equation:

$$\partial_t \bar{u}^1 = (\nu_e^1(t) + \nu)\partial_{zz} \bar{u}^1, \tag{4.6}$$

where $\nu_e^1(t)$ is the time-dependent eddy viscosity for the fundamental mode defined by

$$\nu_e^1(t)\partial_{zz} \bar{u}^1 = -\partial_z [\langle uw \rangle^{xy}]^1. \tag{4.7}$$

This definition, however, is singular where $\partial_{zz} \bar{u}^1 = 0$. Thus, to avoid numerical problems when computing $\nu_e^1$ in the simulations, it is more convenient to use a global definition, based on the evolution equation for the energy $E_{\bar{u}}^1$ of the mode $\bar{u}^1$.
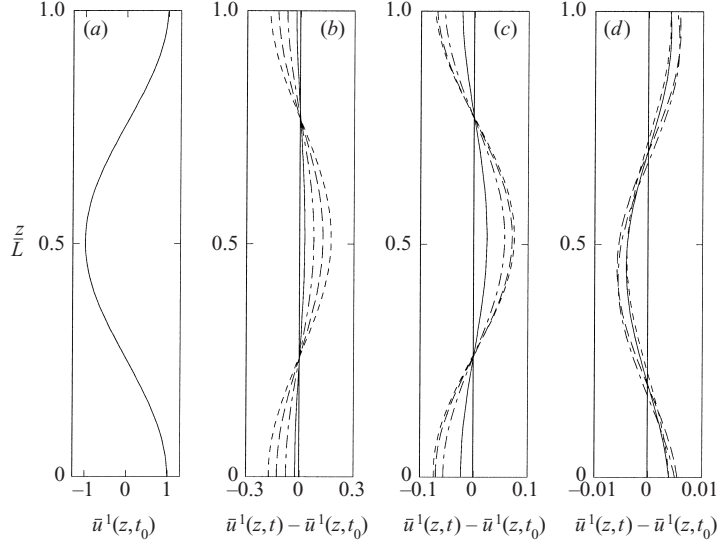
FIGURE 9. Evolution of the fundamental mode $\bar{u}^1$ of the mean flow profile in Simulations ANS, AMS and ASS. Here the velocity scale is $U_0$, the amplitude of the perturbation imposed at $t = t_0$. (a) Profile of $\bar{u}^1$ at $t = t_0$. (b, c, d) Profile of the fundamental profile increment $\bar{u}^1(z, t) - \bar{u}^1(z, t_0)$ at $t = t_0$ (solid line), $t = t_0 + \tau_0$ (dot-dashed curve), $t = t_0 + 2\tau_0$ (long-dashed curve), $t = t_0 + 3\tau_0$ (dashed curve) and $t = t_0 + 4\tau_0$ (dotted curve) in Simulations (b) ANS, (c) AMS and (d) ASS.

Multiplying (4.5) by $\bar{u}^1$ and integrating over the vertical, we obtain

$$\partial_t E_{\bar{u}}^1 + \langle \bar{u}^1 \partial_z \langle uw \rangle^{xy} \rangle^z = \nu \langle \bar{u}^1 \partial_{zz} \bar{u}^1 \rangle^z, \tag{4.8}$$

which may be written as

$$\partial_t E_{\bar{u}}^1 = (\nu_e^1(t) + \nu) \langle \bar{u}^1 \partial_{zz} \bar{u}^1 \rangle^z. \tag{4.9}$$

With periodic boundary conditions, the eddy viscosity $\nu_e^1(t)$ is then given by

$$\nu_e^1(t) = -\frac{\langle \bar{u}^1 \partial_z \langle uw \rangle^{xy} \rangle^z}{\langle \bar{u}^1 \partial_{zz} \bar{u}^1 \rangle^z} = \frac{\langle \bar{u}^1 \partial_z \langle uw \rangle^{xy} \rangle^z}{\langle (\partial_z \bar{u}^1)^2 \rangle^z}, \tag{4.10}$$

which is equivalent to (4.7) but is easier to compute numerically, since $\langle (\partial_z \bar{u}^1)^2 \rangle^z > 0$.

The ensemble-averaged results are plotted on figure 10 for the non-stratified (ANS), moderately stratified (AMS) and strongly stratified (ASS) simulations. We also show the results obtained for each realization in order to highlight the sensitivity of $\nu_e^1(t)$ to the initial velocity field. As the initial turbulence is supposed to be homogeneous, we expect the initial value of $\nu_e^1$ to be zero. This is not exactly the case in each realization, due to a slight inhomogeneity of the velocity field at $t = t_0$. However, the initial homogeneity is verified in the mean and the value of $\nu_e^1(t_0)$ averaged over six realizations is close to zero.

On this plot it is clear how the eddy diffusion of momentum is affected by the stratification. The oscillations of the eddy viscosity in the stratified simulations (AMS and ASS) are qualitatively in agreement with the oscillations of the momentum flux observed is the simulations performed by Gerz *et al.* (1989) when the mean shear and stratification are uniform. Here, we can observe how the eddy viscosity, and thus the mean flow profile, are affected by these oscillations when the mean shear, and thus the turbulent fluxes, are not uniform. In the absence of a stratification (simulation ANS), the eddy viscosity $\nu_e^1$ increases during one or two turnover timescales and remains
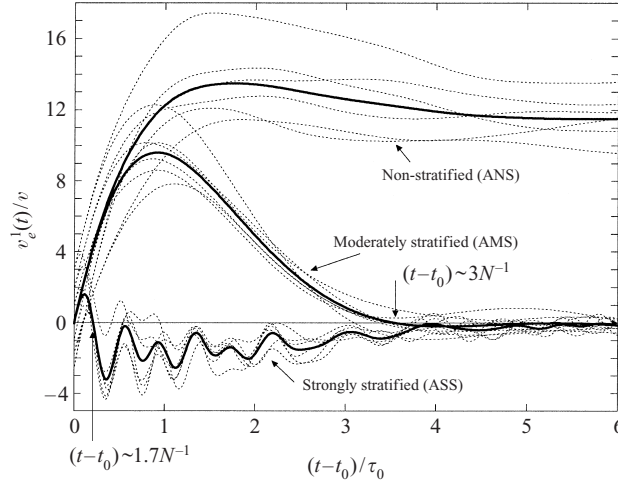
FIGURE 10. Evolution of the eddy viscosity coefficient $v_e^1$ normalized by the molecular viscosity $v$ computed in simulations ANS, AMS and ASS. The time unit is $\tau_0 = l_0/u_0'$, the turnover timescale of turbulence at $t = t_0$. The dotted lines are the results obtained in six realizations of each experiment and the thick lines are the results averaged over the six realizations.

positive throughout the simulation but slowly decreases as turbulence decays. In the moderately stratified simulation, $v_e^1$ starts decreasing earlier ($t - t_0 \simeq 0.9\tau_0 \simeq N^{-1}$) and becomes zero at $t - t_0 \simeq 3.3\tau_0$ ($\simeq 3N^{-1}$). In the strongly stratified simulation (ASS), $v_e^1$ becomes negative at $t - t_0 \simeq 0.2\tau_0$ ($\simeq 1.7N^{-1}$) and remains persistently negative although some oscillations appear, which accounts for the growth of the mean flow energy in Simulation ASS. These results are further discussed in §6.

## 5. Effect of turbulence on a stable mean density profile

### 5.1. *Definition of the simulations*

We now simulate the evolution of the mean density profile $\bar{\rho}(z, t)$ as turbulence decays, when a perturbation is introduced in the initial stratification (associated with the initial mean density profile $\bar{\rho}(z, t_0)$). The isotropic, homogeneous turbulent field $\boldsymbol{u}_{iht}(\boldsymbol{x})$ generated as described in §3 is used as the initial condition for the velocity field with no imposed mean flow. Only the case of zero initial density perturbations is considered (i.e. $E_{\rho'}(t_0) = 0$).

The linear density mean profile is initially perturbed by a fundamental mode with amplitude $\bar{\rho}_{p0}$:

$$\bar{\rho}_p(z, t_0) = \bar{\rho}_{p0} \cos(2\pi z/L). \tag{5.1}$$

The choice of the value of $\bar{\rho}_{p0}$ was made by considering the case of an equipartition between the initial poloidal, toroidal and potential energies:

$$E_{\bar{\rho}} \simeq E_{pol}(t_0) \simeq E_{tor}(t_0) \simeq \tfrac{1}{3} E(t_0), \tag{5.2}$$

which requires $\bar{\rho}_{p0} g/\rho_r N_l u_0' = \sqrt{3}$. The resulting density profile $\bar{\rho}_l + \bar{\rho}_p$ is everywhere stable and the local Brunt–Väisälä frequency $\mathcal{N}$ defined by (2.5) varies initially with height $z$. The minimum and maximum values of $\mathcal{N}(z, t_0)$ will be denoted by $\mathcal{N}_{min}$ and $\mathcal{N}_{max}$.

The Prandtl number $P = v/\kappa$ is taken equal to unity and we use again two values of
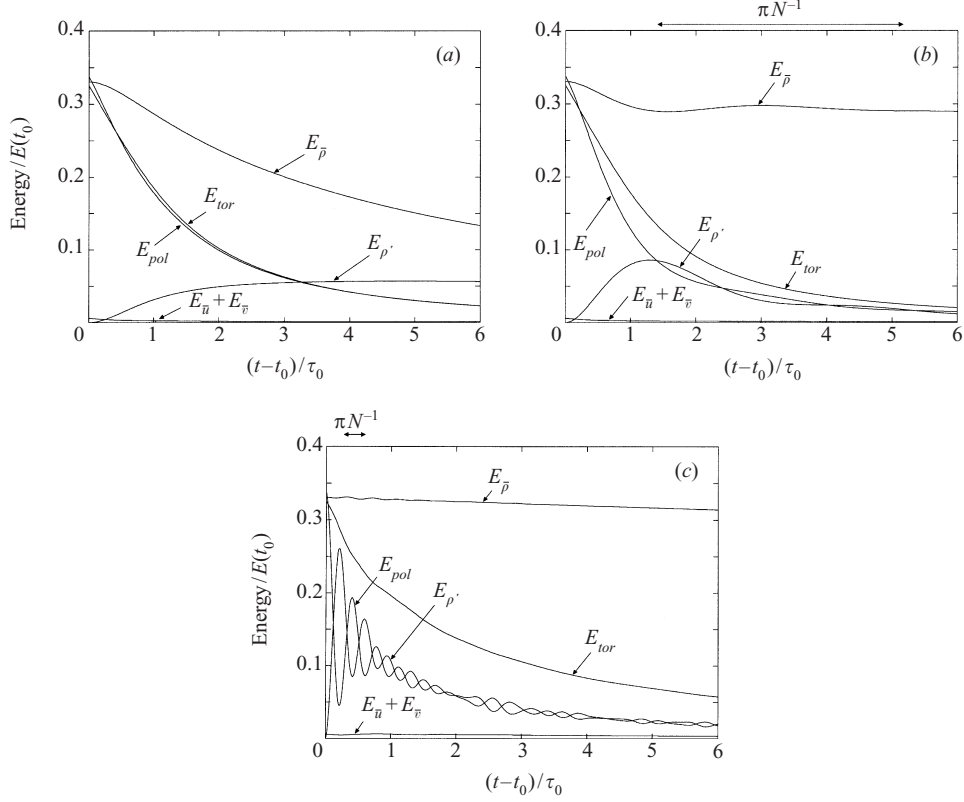
FIGURE 11. Evolution of energies $E_{pol}$, $E_{tor}$, $E_{\bar{u}} + E_{\bar{v}}$, $E_{\rho'}$ and $E_{\bar{\rho}}$ in Simulations (a) BNS, (b) BMS and (c) BSS. In these simulations, $E_{\bar{\rho}} \simeq E_{pol} \simeq E_{tor}$ and $E_{\rho'} = 0$ initially. The time unit is $\tau_0 = l_0/u_0'$, the turnover timescale of turbulence at $t = t_0$.

the Froude number: $Fr = 1.2$ (moderately stratified simulation BMS) and $Fr = 0.12$ (strongly stratified simulation BSS). A measure of the vertical variations of the Brunt–Väisälä frequency is provided by the value of $\mathcal{N}_{max}/N$. We have $\mathcal{N}_{max}/N = 1.4$ in Simulation BMS and $\mathcal{N}_{max}/N = 1.05$ in Simulation BSS.

A non-stratified simulation (BNS) was also performed ($Fr = \infty$). In this case, variable $\rho$ simply plays the role of a passive scalar being mixed by turbulence without affecting the flow dynamics. Thus, the flow field is simply the continuation of the precomputation run. In the initial condition, the periodic component of the mean density profile is still given by (5.1) and the background linear profile is zero.

The definition of the simulations is summarized in table 2.

### 5.2. Evolution of the turbulent and mean quantities

The energies $E_{pol}$, $E_{tor}$, $E_{\bar{u}} + E_{\bar{v}}$, $E_{\rho'}$ and $E_{\bar{\rho}}$ are plotted as a function of time on figure 11 for each simulation.

On these plots, the time unit is $\tau_0 = l_0/u_0'$ and all the energies are normalized by the initial total energy at $t = t_0$. Although several realizations of these numerical experiments have been performed, we only show the results for one realization because all the flow diagnostics were found to evolve similarly for each realization.

When $\rho$ is a passive scalar (non-stratified simulation BNS), $E_{\bar{\rho}}$ decreases mono-

tonically as time evolves.† In this case, the effect of the turbulent mixing is to damp the initial perturbation in the density profile, while the turbulent density fluctuations increase monotonically. In the stratified simulations (BMS and BSS), oscillations of the poloidal energy $E_{pol}$ and potential energy $E_{\rho'}$ are again observed on a timescale of order $\pi N^{-1}$. The toroidal energy $E_{tor}$ decreases slowly in these stratified simulations whereas isotropy is conserved in the non-stratified case BNS ($E_{pol}(t) \simeq E_{tor}(t)$) since the density field has no effect on the flow field. After six turnover timescales, $E_{tor}/E_{pol} \simeq 3.3$ in the strongly stratified simulation (BSS) and $E_{tor}/E_{pol} \simeq 1.5$ in the moderately stratified simulation (BMS). This result confirms the tendency to anisotropy of stratified turbulence and the presence of vortical structures with a weak vertical velocity component, whereas the poloidal energy $E_{pol}$ and the potential energy $E_{\rho'}$ are low and equipartitioned for large times. After six turnover timescales, the ratio $(E_{pol} + E_{\rho'})/E_{tor}$ is 1.3 in the moderately stratified simulation BMS and 0.7 in the strongly stratified simulation BSS. As was already observed in the simulations of stratified shear flows AMS and ASS, the toroidal energy is dissipated faster in the moderately stratified case than in the strongly stratified case (after six turnover timescales $E_{tor} \simeq 0.02E(t_0)$ in Simulation BMS whereas $E_{tor} \simeq 0.06E(t_0)$ in Simulation BSS).

Let us now focus on the evolution of the mean quantities. The mean flow energy $E_{\bar{u}} + E_{\bar{v}}$ remains negligible compared to the other energies in all cases, but a significant increase and weak amplitude oscillations of the potential energy $E_{\bar{\rho}}$ are observed in the stratified simulations (BMS and BSS) as soon as the fluid particles are subject to the restoring buoyancy forces ($t - t_0 \simeq 1.25N^{-1}$ in Simulation BMS and $t - t_0 \simeq N^{-1}$ in Simulation BSS). The initial perturbation of the mean density profile is thus alternately damped and amplified, so that $E_{\bar{\rho}}$ is the major remaining component of the energy at the end of the stratified simulations. After six turnover timescales, $E_{\bar{\rho}}/E_{\bar{\rho}}(t_0) \simeq 0.95$ in Simulation BSS and $E_{\bar{\rho}}/E_{\bar{\rho}}(t_0) \simeq 0.85$ in Simulation BMS, whereas $E_{\bar{\rho}}/E_{\bar{\rho}}(t_0) \simeq 0.4$ in the non-stratified simulation.

The profiles of $\bar{\rho}$ are plotted on figure 12 for $(t - t_0) = 4\tau_0$ and a zoom of figures 11($a$), 11($b$) and 11($c$) is provided on figure 13($a$).

We have also plotted the solution for $E_{\bar{\rho}}$ when the effect of the turbulence is ignored (this corresponds to the purely diffusive decay of the mean density profile). As for the mean flow profile (see §4.2), the periodic mean density profile $\bar{\rho}_p(z, t)$ may be decomposed as

$$\bar{\rho}_p(z, t) = \bar{\rho}_p^1(z, t) + \bar{\rho}_p^{>1}(z, t), \tag{5.3}$$

where $\bar{\rho}_p^1$ is the fundamental mode (imposed at $t = t_0$), and $\bar{\rho}_p^{>1}$ is the sum of the harmonics with wavenumbers greater than $2\pi/L$. The potential energy $E_{\bar{\rho}}$ of the mean density profile is

$$E_{\bar{\rho}}(t) = E_{\bar{\rho}}^1 + E_{\bar{\rho}}^{>1}, \tag{5.4}$$

where $E_{\bar{\rho}}^1 = (1/2)(g/\rho_r N)^2 \langle (\bar{\rho}_p^1)^2 \rangle^z$ and $E_{\bar{\rho}}^{>1} = (1/2)(g/\rho_r N)^2 \langle (\bar{\rho}_p^{>1})^2 \rangle^z$. The energy $E_{\bar{\rho}}^{>1}$ (figure 13$b$) grows until $(t - t_0) \simeq 3.5\tau_0$ in the non-stratified case and then slowly decreases whereas in the stratified simulations its evolution is subject to the oscillations induced by the stable stratification. In the moderately stratified simulation (BMS), its maximum value is of the same order as in the non-stratified simulation (of order $10^{-3}E(t_0)$), whereas in the strongly stratified simulation (BSS) it is much lower (of

---

† Note that in the non-stratified case the term 'potential energy' is not appropriate and may be replaced by 'variance'. In this case, the only energy scale is the initial kinetic energy of the flow field. $E_{\rho'}$ is then defined as $E_{\rho'}(t) = E_{kin}(0)\langle \rho'^2 \rangle^{xyz}/\rho_r^2$ and $E_{\bar{\rho}}$ is defined as $E_{\bar{\rho}}(t) = E_{kin}(0)\langle \bar{\rho}_p^2 \rangle^z/\rho_r^2$.
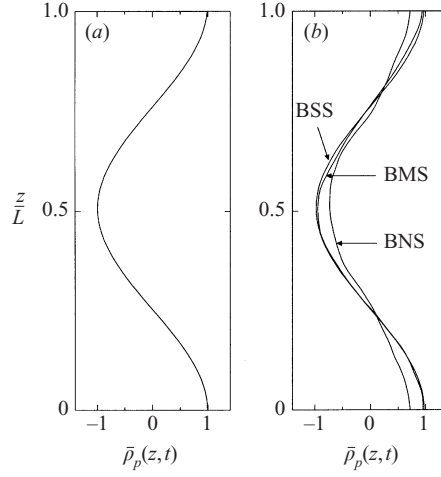
FIGURE 12. Periodic component $\bar{\rho}_p$ of the mean density profile in Simulations BNS, BMS and BSS. Here the density scale is $\bar{\rho}_{p0}$, the amplitude of the perturbation imposed at $t = t_0$. (a) $t = t_0$. (b) $t = t_0 + 4\tau_0$.
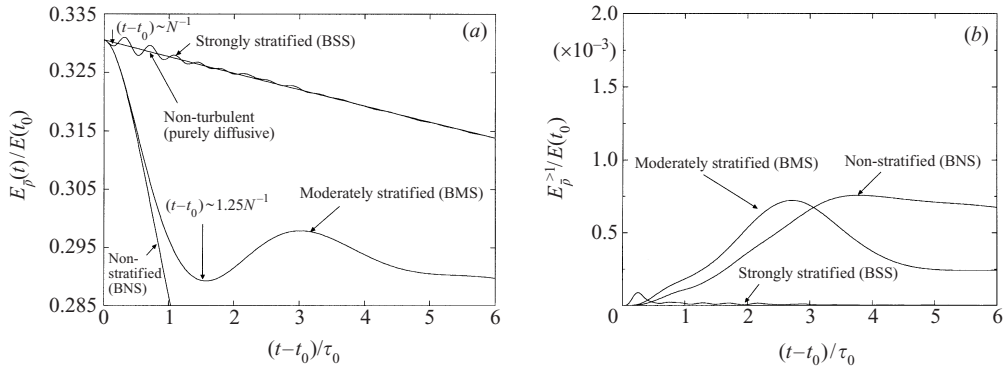


FIGURE 13. Evolution of (a) $E_{\bar{\rho}}$, the energy of the mean density profile and (b) $E_{\bar{\rho}}^{>1}$, the energy of the harmonics with wavenumbers $> 2\pi/L$ in simulations BNS, BMS and BSS. The time unit is $\tau_0 = l_0/u'_0$, the turnover timescale of turbulence at $t = t_0$. For comparison, the analytical solution for $E_{\bar{\rho}}(t)$ has been plotted when the effect of turbulence is ignored (purely diffusive decay).

order $10^{-4}E(t_0)$). Thus, $E_{\bar{\rho}}^{>1}$ remains much lower than the energy of the fundamental in all simulations, and $E_{\bar{\rho}} \simeq E_{\bar{\rho}}^1$ at any time.

Figure 13(a) clearly shows the oscillations of the mean density profile energy $E_{\bar{\rho}}$ in the stratified simulations. The oscillations are faster in the strongly stratified simulation (BSS) but their amplitude is larger in the moderately stratified simulation (BMS). In the strongly stratified case, $E_{\bar{\rho}}$ becomes greater than the purely diffusive solution after a period of $\simeq 0.25\tau_0$ ($\simeq 2N^{-1}$) and then oscillates with a mean rate of decay equal to the diffusive rate. Thus, the turbulent vertical fluctuations are rapidly damped by the strong stratification, which reduces dramatically the turbulent vertical mass transport. In the moderately stratified simulation (BMS), the vertical turbulent motions are damped more slowly so that the turbulent mass transport remains efficient until $(t - t_0) \simeq 1.5\tau_0$ ($\simeq 1.25N^{-1}$). As a consequence, the final value of $E_{\bar{\rho}}$ remains lower than the diffusive solution in spite of the oscillation occurring at $(t - t_0) \simeq 1.25N^{-1}$.
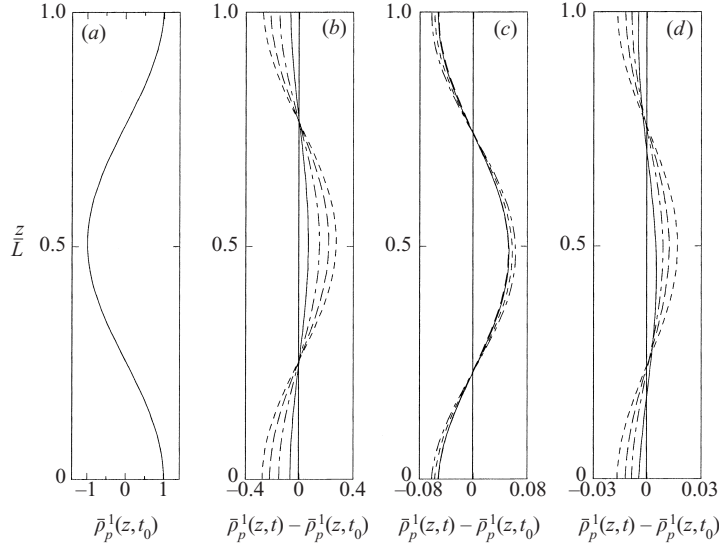
FIGURE 14. Evolution of the fundamental mode $\bar{\rho}_p^1$ of the mean density profile perturbation in Simulations BNS, BMS and BSS. Here the density scale is $\bar{\rho}_{p0}$, the amplitude of the perturbation imposed at $t = t_0$. (*a*) Profile of $\bar{\rho}_p^1$ at $t = t_0$. (*b,c,d*) Profile of the fundamental perturbation increment $\bar{\rho}_p^1(z,t) - \bar{\rho}_p^1(z,t_0)$ at $t = t_0$ (solid line), $t = t_0 + \tau_0$ (dot-dashed curve), $t = t_0 + 2\tau_0$ (long-dashed curve), $t = t_0 + 3\tau_0$ (dashed curve) and $t = t_0 + 4\tau_0$ (dotted curve) in Simulations (*b*) BNS, (*c*) BMS and (*d*) BSS.

### 5.3. *Eddy diffusion of buoyancy*

The evolution of the mean density perturbation can be traced from the profiles of $\bar{\rho}_p^1(z,t) - \bar{\rho}_p^1(z,t_0)$ plotted on figure 14 at times $(t - t_0) = \tau_0$, $2\tau_0$, $3\tau_0$ and $4\tau_0$.

These plots allow us to observe that in all cases the fundamental mode $\bar{\rho}_p^1$ has almost constant spatial phase, although a very weak vertical shift is observed in the stratified simulations. This small shift is presumably due to the large-scale wavy oscillations induced by the buoyancy forces. However, the final density profile is roughly in phase with the initial profile. Thus, as for the mean flow in Simulations A (see §4.3), the equation for $\bar{\rho}_p^1$

$$\partial_t \bar{\rho}_p^1 + \partial_z [\langle \rho' w \rangle^{xy}]^1 = \kappa \partial_{zz} \bar{\rho}_p^1 \qquad (5.5)$$

(where $[\langle \rho' w \rangle^{xy}]^1$ is the fundamental mode of the vertical profile of the buoyancy flux) may be replaced by the following diffusion equation:

$$\partial_t \bar{\rho}_p^1 = (\kappa_e^1(t) + \kappa) \partial_{zz} \bar{\rho}_p^1. \qquad (5.6)$$

Here, $\kappa_e^1(t)$ is the time-dependent eddy diffusivity for the fundamental mode, which with periodic boundary conditions can be defined as

$$\kappa_e^1(t) = -\frac{\langle \bar{\rho}_p^1 \partial_z \langle \rho w \rangle^{xy} \rangle^z}{\langle \bar{\rho}_p^1 \partial_{zz} \bar{\rho}_p^1 \rangle^z} = \frac{\langle \bar{\rho}_p^1 \partial_z \langle \rho w \rangle^{xy} \rangle^z}{\langle (\partial_{zz} \bar{\rho}_p^1)^2 \rangle^z}. \qquad (5.7)$$

The eddy diffusivity has been computed in simulations BNS, BMS and BSS (figure 15).

The oscillations of $\kappa_e^1$ are again qualitatively consistent with the oscillations of the buoyancy fluxes observed in the simulations of Gerz *et al.* (1989) in unsheared stratified turbulence when the stratification is uniform. Here, the evolution of the eddy diffusivity shows how the mean density profile is affected when a perturbation
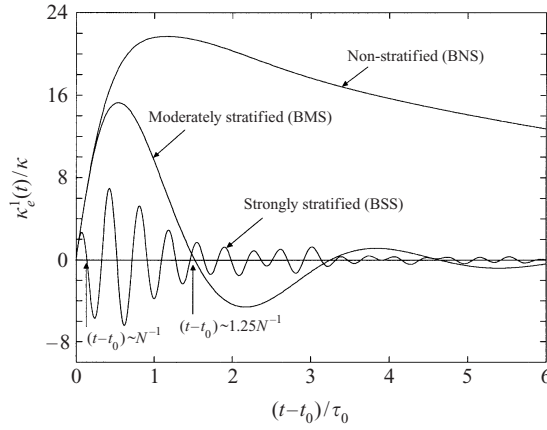
FIGURE 15. Evolution of the eddy diffusivity coefficient $\kappa_e^1$ normalized by the molecular diffusivity $\kappa$ computed in simulations BNS, BMS and BSS. The time unit is $\tau_0 = l_0/u_0'$, the turnover timescale of turbulence at $t = t_0$.

is introduced in the initial condition. In all three simulations, BNS, BMS and BSS, the initial value of $\kappa_e^1$ is zero since there are no density fluctuations at $t = t_0$. In the non-stratified simulation, the eddy diffusivity grows as turbulence evolves and reaches a maximum value after one turnover timescale. Then it starts decreasing slowly as the turbulent motions decay and lose their mixing efficiency. The maximum is reached earlier ($t - t_0 \simeq 0.5N^{-1}$) in both stratified simulations and $\kappa_e^1$ becomes negative at $t - t_0 \simeq 1.25N^{-1}$ in Simulation BMS and $t - t_0 \simeq N^{-1}$ in Simulation BSS. This causes the mean density perturbation to grow and explains the first oscillation of $E_{\bar{\rho}}$ observed on figure 13($a$). For long times, the behaviour of the eddy diffusivity is merely oscillatory in both the strongly stratified and moderately stratified simulations.

## 6. Discussion

### 6.1. *Short-time evolution of the mean profiles*

In this section, we discuss the evolution of the mean flow profile in Simulations AMS and ASS, and of the mean density profile in Simulations BMS and BSS in the first stages of the decay (over a time of order $N^{-1}$).

The evolution of the mean flow in Simulations ASS and AMS shows that the presence of a strong stratification greatly modifies the turbulence–mean flow interaction compared to the moderately stratified case. It seems that a competition takes place between the classical eddy diffusion of momentum and the counter-gradient momentum fluxes induced by the restoring buoyancy forces. The latter dominates when the stratification is strong enough and causes the mean flow perturbation to grow after a short period of time (Simulation ASS, figure 8$a$), whereas in the moderately stratified simulation, the effect of the stratification is simply to reduce the vertical transport and to slow down the decay of the mean flow energy (Simulation AMS, figure 8$a$).

The evolution of a mean current in the presence of a turbulent field and strong stratification has also been investigated experimentally by Spedding (1997) and Bonnier (1999) for instance. In these experiments, a sphere is towed horizontally (say, along the $x$-axis) in strongly stratified water (see also Lin & Pao 1979). The intensity of the defect velocity in the turbulent wake is measured downwind and its spatial

evolution behind the sphere can be described in terms of temporal evolution in the initial value problem of decaying turbulence. The main difference between our numerical simulations and these experiments is the horizontal invariance of the mean flow along the $y$-coordinate, whereas the wake of a sphere has some strong variations along that direction. Nevertheless, the evolution of the defect velocity in these laboratory experiments has some aspects similar to our numerical simulations. From his measurements, Spedding (1997) found a change in the rate of decay of the defect velocity after a time period of order $1.7N^{-1}$. Then, he observed that the turbulent wake loses its three-dimensional features and that the defect velocity starts decreasing more slowly than in the near wake. However, it is not clear from these experiments whether this change in the mean flow decay is associated with an input of energy to the mean current or is simply due to the damping of the turbulent fluxes under the effect of the stratification. In the experiments of Bonnier (1999), an acceleration of the mean current is indeed detected (after a time lapse of order $2.3N^{-1}$), which indicates that a net energy transfer occurs from the turbulent motion to the mean motion by the way of the restoring buoyancy forces.

From these laboratory experiments and our numerical simulations, it is clear that the mean flow decay strongly depends on the intensity of the stratification. The change in the turbulence–mean flow interaction (compared to the non-stratified case) may be associated with the beginning of the so-called 'collapse' of the velocity field, although many definitions of the collapse are used in the literature, depending on specific flow configurations. Here, we may define the 'collapse' as the moment at which the eddy viscosity (as defined in §4.3) becomes zero. This happens at $1.7N^{-1}$ in Simulation ASS and $3N^{-1}$ in Simulation AMS (see figure 10). This characteristic timescale is in good agreement with many observations in grid turbulence (e.g. Lienhard & Van Atta 1990) or turbulent wakes (Hopfinger, Flór & Bonneton 1991; Chomaz, Bonneton & Hopfinger 1993; Spedding 1997; Bonnier 1999), in which the 'collapse' occurs after a period of order $2N^{-1}$.

It is important to emphasize that the mean flow does not comprise part of the vortical component in the flow decomposition, and that its growth in Simulation ASS occurs after a short period of time. These two remarks show that the acceleration of the mean current cannot be attributed to the classical inverse cascade to the large-scale vortical structures which takes place over a much longer period of time. This tendency may be explained by the linear processes, which dominate the nonlinear processes in the first stage of decay of turbulence using a slightly non-homogeneous version of the rapid distortion theory (Galmiche & Hunt 2002): under conditions of strong stratification, the linear equations of motion can be solved for short times when initially homogeneous and isotropic turbulence interacts with a horizontal mean flow profile. The linear computation of the momentum fluxes then shows that the mean flow is indeed subject to a time-dependent eddy viscosity which becomes negative after a time period of $\sqrt{3}N^{-1} \simeq 1.73N^{-1}$. This is in fairly good agreement with our strongly stratified simulation ASS.

We see in Simulations BMS and AMS that in the case of a moderate stratification, the short-time evolution of a perturbation in the mean density profile (Simulation BMS, figure 13$a$) is more affected by the buoyancy forces than the evolution of a perturbation in the mean flow profile (Simulation AMS, figure 8$a$): whereas the decay of the mean flow energy $E_{\bar{u}}$ is monotonic in Simulation AMS, an increase of the mean potential energy $E_{\bar{\rho}}$ is observed in Simulation BMS at time $1.25N^{-1}$, which shows that a significant amount of potential energy is transferred from the turbulent field $\rho'$ to the mean field $\bar{\rho}$. In the strongly stratified simulation BSS, this energy exchange

happens faster (at $N^{-1}$) but has a much lower amplitude due to the strong reduction of the vertical motions of the fluid particles.

In the unsheared simulations BMS and BSS, the 'collapse' may be defined for the density field as the time at which the eddy diffusivity (as defined in § 5.3) becomes zero. This happens at about $1.25N^{-1}$ in Simulation BMS and $N^{-1}$ in Simulation BSS (see figure 15). Thus, the 'collapse' of the density field in Simulations BMS and BSS occurs earlier than the collapse of the velocity field observed in Simulations AMS and ASS. Within the framework of the rapid distortion theory, the short-time computation of the buoyancy fluxes in decaying turbulence with homogeneous and isotropic initial conditions, subjected to a strong, non-uniform stratification, shows that the mean density profile is subjected to a time-dependent eddy diffusivity which becomes negative at $\sqrt{15/16}N^{-1} \simeq N^{-1}$ (Galmiche & Hunt 2002). This is close to the collapse time found in the strongly stratified simulation BSS.

### 6.2. *Long-time evolution of the mean density profile*

Here we discuss the evolution of the mean density profile in Simulations BMS and BSS over a few turnover time scales.

In figure 15 we note that the collapse of the eddy diffusivity as defined in the previous section is followed by some persistent oscillations in both the moderately (BMS) and strongly stratified (BSS) simulations, which can be traced back to oscillating exchanges of potential energy between the turbulent field and the mean field.

The time-averaged value of $\kappa_e^1/\kappa$ over a few turnover timescales is slightly positive in the moderately stratified simulation BMS (of order 2) and roughly zero in the strongly stratified simulation (BSS). Thus, compared to the non-stratified simulation BNS, the time-averaged effect of the buoyancy forces in the stratified simulations is to inhibit the turbulent diffusion of mass.

We may compare this result with some laboratory experiments of decaying turbulence (e.g. Park *et al.* 1994; Pearson & Linden 1983). In these experiments, density layers appear in the final stage of decay of turbulence in a fluid that is initially uniformly stratified, which means that small perturbations in the mean density profile grow as turbulence evolves and finally form persistent horizontal layers due to the local turbulent mixing. In our Simulations BMS and BSS, the collapse of the density field (as defined in § 6.1) can be traced back to this tendency for short times, and the long-time behaviour of the potential energy $E_{\bar{\rho}}$ (figure 13a) shows that the decay of the mean profile $\bar{\rho}(z, t)$ is indeed much slower than in the non-stratified simulation. However, we do not observe any persistent growth of the perturbation in the mean density profile. The reason is probably that in our simulations at low Reynolds number, the flow decays rapidly and the turbulent fluxes are damped before persistent layers have time to develop. This is a significant difference with the experiments of Park *et al.* (1994), in which the turbulence is generated by moving a vertical rod back and forth in a water tank stratified in salinity, and density layers form after numerous stirring events, when the turbulence is well-developed. The long-time action of the nonlinear processes certainly plays a major role in the formation of permanent density layers in forced turbulence. Moreover, in these laboratory experiments, the density layers first form close to the top and bottom boundaries of the tank and expand slowly into the interior. Thus, the experimental boundary conditions may also play a significant role in the formation of layers, which cannot be reproduced in our numerical simulations with periodic boundary conditions. It is also possible that, as suggested by Pearson & Linden (1983), the density layers observed in the final stage of decay of turbulence result from an equilibrium between the viscous dissipation and

the buoyancy forces, and only develop at high Prandtl number, e.g. $P \simeq 800$ in salted water (whereas $P = 1$ in our simulations).

### 6.3. *Long-time evolution of the mean flow profile*

Here we discuss the evolution of the mean flow profile in Simulations AMS and ASS over a few turnover timescales.

Unlike the eddy diffusivity in Simulations BMS and BSS, there is a qualitative difference between the large-time behaviour of the eddy viscosity in the strongly stratified (ASS) and moderately stratified (AMS) simulations. When the stratification is moderate, the eddy viscosity remains zero for large times with almost no oscillations. On the contrary, when the stratification is strong, the collapse of the velocity field is followed by a persistent, oscillatory acceleration of the mean current. In Simulation AMS, the averaged value of $v_e^1/v$ over a few turnover timescales is small but positive (of order 3), whereas it is negative (of order $-1.5$) in Simulation ASS.

There is no clear experimental evidence of a persistent acceleration of the mean current over a long period of time in turbulent wakes of bodies or other stratified turbulent shear flows. On the other hand, the presence of shear layers has been observed in the final stage of decay of turbulence in several laboratory experiments with no imposed mean shear initially (e.g. Pearson & Linden 1983), which suggests that initial perturbations in the mean flow profile are indeed amplified by the counter-gradient turbulent fluxes. It may be interesting to undertake further experimental investigations to describe accurately the behaviour of the horizontal mean current in a turbulent shear flow as a function of the intensity of the stratification.

From a general point of view, it is important to identify the interactions that may be responsible for the persistent growth of the mean flow. We note in figure 5 that the growth of the mean flow in the strongly stratified simulation is accompanied by persistent oscillations of the poloidal and potential energies. In the low-Froude-number limit, the poloidal component of the flow field (with zero vertical vorticity) may be associated with the waves, and the toroidal component (with zero vertical velocity) may be associated with the vortical modes (see Riley *et al.* 1981). From this point of view, we can associate the oscillations observed in Simulation ASS with the presence of a slowly dissipated wave field, which may play a significant role in the time evolution of the mean current. Let us write the evolution equation for the mean flow $\bar{u}(z,t)$ again:

$$\partial_t \bar{u} = -\partial_z \langle uw \rangle^{xy} + v \partial_{zz} \bar{u}. \tag{6.1}$$

Provided that the vertical component $w$ of the velocity field is only associated with the wave field, it is clear from this equation that only the interactions involving at least one wave mode are able to affect the time evolution of the mean flow, namely: (i) the wave–mean flow interactions, (ii) the wave–wave interactions and (iii) the wave–vortical interactions.

The wave–mean flow interaction (i) has already been extensively studied in numerous theoretical studies (e.g. Garrett 1968; Phillips 1968; Andrews & McIntyre 1978; Müller 1976; Grimshaw 1984). Müller (1976) has studied the diffusion of momentum and mass by a weakly nonlinear wave field under WKB assumptions. He treated the cross-coupling of wave distortion and mean field evolution as a small perturbation problem and concluded that the wave field does not induce any vertical transport of buoyancy but does induce a vertical transport of momentum. He found that the wave-induced viscosity had a positive, and even high, value compared to the effective viscosity associated with eddies. However, in his analysis, the mean current had

weak amplitude and the wave field was only smoothly distorted by the mean shear. There are some situations where the waves are strongly distorted by the mean shear. Then, the waves can either be trapped by the mean flow or reach a critical level and eventually accelerate the mean current. For instance, Winters & D'Asaro (1994) have observed in direct numerical simulations that a significant amount of energy was transferred from the wave field to the mean flow near a critical level. Some further investigations are needed to study the interaction of the turbulence-induced waves and the mean current in strongly stratified turbulent shear flows.

Concerning interactions (ii) and (iii), resonant triads of wave modes and vortical modes have been studied by Lelong & Riley (1991) under conditions of strong stratification, but in the absence of a vertical mean shear. Few studies have paid attention to the triads involving an energy transfer to a horizontal mean flow mode, i.e. a mode with vertical wave-vector. It has been pointed out by Galmiche *et al.* (2000) that the interaction of two wave modes with wave-vectors $k_A$ and $k_B$ (and wavenumbers $k_A$ and $k_B$) can give rise to a horizontal mean flow provided that $k_A + k_B$ (or $k_A - k_B$) is vertical and $k_A \neq k_B$. This is another possible mechanism involved in the stratified turbulence–mean flow interaction. To our knowledge, there is no result in the literature on triads involving a vortical mode, a wave mode and a horizontal mean flow mode.

## 7. Summary and concluding remarks

The aim of this paper was to study some aspects of turbulence–mean field interactions in stratified fluids. We have performed direct numerical simulations of freely decaying turbulence in the presence of a stable stratification when either an initial non-uniform vertical mean shear profile or an initial non-uniform density profile is imposed initially. The results of these numerical simulations may be summarized as follows.

(i) When a moderate stratification is applied to a mean flow profile $\bar{u}(z)$ in the presence of an initial turbulent velocity field (Simulation AMS, $Fr = 1.2$), the effect of the buoyancy forces on the fluid particles reduces the vertical transport of momentum and causes the mean flow energy to decay much slower than in the non-stratified case. This phenomenon has been described by defining an eddy viscosity which becomes zero after about $3N^{-1}$ and remains roughly zero for large times. This may be seen as the 'collapse' of the velocity field.

(ii) When a strong stratification is applied (Simulation ASS, $Fr = 0.12$), the eddy viscosity become zero after about $1.7N^{-1}$ and remains persistently negative for large times, which shows that the collapse not only reduces the vertical transport of momentum but also induces an energy transfer from the turbulent field to the mean flow.

(iii) The evolution of an initial perturbation in the mean density profile $\bar{\rho}(z)$ in the presence of a turbulent field is affected by the buoyancy forces and the eddy diffusivity becomes zero at about $1.25N^{-1}$ when a moderate stratification is applied (Simulation BMS, $Fr = 1.2$). Then, the energy of the perturbation increases significantly, which shows that some potential energy is transferred from the turbulent field to the mean field and may be seen as the collapse of the density field. The time-averaged value of the eddy diffusivity over a few turnover timescales is positive but small.

(iv) When the background stratification is strong (Simulation BSS, $Fr = 0.12$), the energy of the perturbation in the mean density profile oscillates around the purely diffusive solution and is thus almost unaffected by the turbulence at large times. The

eddy diffusivity becomes zero at about $N^{-1}$. This may be seen as the collapse of the density field but the eddy diffusivity oscillates during several turnover timesscales with a time-averaged value of order zero.

In the strongly stratified simulations, the growth of the mean profiles for short times can be traced back to the *tendency* of stratified turbulence to form horizontal layers and can be explained by the linear processes which are dominant in the first stage of decay of turbulence (Galmiche & Hunt 2002). This suggests that the formation of layers in stratified flows may be described in terms of turbulence–mean field interactions, an approach that complements other studies describing layer formation in terms of anisotropy (e.g. Godeferd & Cambon 1994) or in terms of vortex pair, zig-zag instability (Billant & Chomaz 2000).

The Simulations BMS and BSS highlight the effect of the stratification on the eddy diffusivity. However, they do not allow us to reproduce the formation of persistent density layers as observed in laboratory experiments (e.g. Park *et al.* 1994; Pearson & Linden 1983). Some further investigations are needed to explain the persistent growth of a perturbation in the mean density profile, as described by Phillips (1972) and Posmentier (1977) with heuristic arguments. In particular, the effect of high Reynolds number, high Prandtl number and rigid boundary conditions may play a significant role in the laboratory experiments such as those of Park *et al.* (1994).

On the other hand, the negative value of the eddy viscosity over several turnover timescales in Simulation ASS does indicate that persistent shear layers develop when the stratification is strong. The effect of the stratification on the mean flow is more dramatic than suggested by Phillips (1972), who expected that the eddy viscosity would be strongly reduced by the buoyancy forces but keep positive values even in strongly stratified turbulence. In our Simulation ASS, the growth of the mean flow is not a consequence of the slow inverse cascade to the large-scale vortical motions, but is the result of a rapid energy transfer (on a timescale of order $N^{-1}$) from the turbulent field to the mean flow component, which cannot be included either in the wave or in the vortex component of the flow decomposition.

It is important to emphasize that the evolution of the eddy viscosity $v_e^1(t)$ and diffusivity $\kappa_e^1(t)$ as defined in our simulations is only a diagnostic which can be traced back to the behaviour of the fundamental modes of the perturbations in the mean profiles (imposed in the initial condition) with periodic boundary conditions. The results from the rapid distortion theory (Galmiche & Hunt 2001) show that the concepts of (time-dependent) eddy viscosity and diffusivity are indeed relevant for short times, as long as the effects of nonlinear processes are weak. In our simulations, the description of the mean quantities in terms of eddy viscosity and diffusivity is also relevant for large times since the small-scale harmonics in the mean profiles are only slightly influenced by the turbulent field and only the fluctuations of the fundamental modes are significant. However, the evolution of the mean profiles may not be modelled by a diffusion equation in the more complex flows encountered in realistic situations, in particular when complex boundary conditions have to be taken into account. Wave–mean flow interactions may play a more significant role in high-Reynolds-number and/or forced turbulence than in our simulations, and generate small scales in the mean profiles when critical levels are reached. Furthermore, large-scale modes with quasi-vertical wave-vector that correspond to quasi-horizontal fluid motions (not included in the mean flow mode) and may play an important role in real stratified turbulence, are particulalry difficult to represent in spectral codes even with higher resolution.

From this point of view, laboratory experiments are necessary to study small-scale processes. Although simulations with higher resolution are useful as validation runs, it is still impossible to simulate high-Reynolds-number real flows with no parameterization. However, the present study shows that simulations with moderate resolution highlight some fundamental features of stratified turbulence and are a good starting point for theoretical analysis: based on the results of the present study, an analytical, linear model has been proposed by Galmiche & Hunt (2002) for short times, that is in good agreement with the simulations but does not include any low-Reynolds-number assumption. Therefore, our results seem to reflect some quite general properties of stratified turbulent flows. The reader is referred to Galmiche & Hunt (2002) on this point. At large time, the turbulence–mean field interaction may be different, but probably stronger in high-Reynolds-number real flows, as the kinetic energy is dissipated more slowly.

There are a few other points which may require further investigations. First, the effect of non-zero density fluctuations (i.e. non-zero $E_{\rho'}(t_0)$), correlated or not to the initial velocity field, has not been considered here. According to the RDT model of Hanazaki & Hunt (1996), the linear processes involved in the turbulence–mean flow interaction should not be affected by initial density fluctuations in the first stage of decay of turbulence. On the other hand, the temporal oscillations in the buoyancy flux should change phase, which may affect the short-time behaviour of density layers. However, many laboratory experiments show that for large time, layers form in the final stage of decay of turbulence independently of the details of the initial condition (e.g. Pearson & Linden 1983). Another question is how the turbulence–mean field is affected by the lengthscale of the perturbations in the mean fields compared to the lengthscale of turbulence. The short-time solution provided by RDT (Galmiche & Hunt 2002) shows that the interaction is strongest and layers form when the mean fields vary on a lengthscale of order $u'_0/N$. This is also consistent with the experiments of Park *et al.* (1994) and with atmospheric observations (Hunt, Kaimal & Gaynor 1985).

To further study the turbulence–mean field interactions in stratified media, it would be interesting to simulate the evolution of the mean flow and mean density profiles when the turbulence is forced by a random input of energy. When, as in previous studies (e.g. Herring & Métais 1989), the forced simulations are initialized with a turbulent field with no mean shear and uniform stratification, the mean flow profile $\bar{u}$ and the mean density profile $\bar{\rho}$ remain unaffected. When the mean profiles are initially perturbed, the constant input of energy to the turbulent field might induce constantly counter-gradient, non-uniform turbulent fluxes affecting the mean profiles and leading the flow to a steady state where the eddy diffusion of mass an momentum is balanced by the dissipative processes.

In conclusion, these numerical simulations highlight some fundamental properties of stratified turbulence and its interaction with the mean flow and density fields. From a practical point of view, the understanding of these properties is necessary to improve the parametrization of small scales in models of large-scale flows in oceans or atmospheres where the effect of the stratification is preponderant. Although a number of results are available from the stability theory that highlight the tendency of stratified flows to develop counter-gradient fluxes, numerical simulations and laboratory experiments are necessary because real flows generally do not satisfy small-perturbation assumptions. Some new questions may arise when the effects of an external forcing, rotation or complex boundary conditions are taken into account.

## REFERENCES

ANDREWS, D. G. & MCINTYRE, M. E. 1978 An exact theory of nonlinear waves on a Lagrangian-mean flow. *J. Fluid Mech.* **89**, 4, 609–646.

BILLANT, P. & CHOMAZ, J. M. 2000 Theoretical analysis of the zigzag instability of a vertical columnar vortex pair in a strongly stratified fluid. *J. Fluid Mech.* **419**, 29–63.

BONNIER, M. 1999 Sillage d'une sphère en milieu linéairement stratifié. Caractérisation des structures tourbillonnaires. PhD Dissertation, Institut National Polytechnique de Toulouse.

CHOMAZ, J. M., BONNETON, P. & HOPFINGER, E. J. 1993 The structure of the near wake of a sphere moving horizontally in a stratified fluid. *J. Fluid Mech.* **254**, 1–21.

CORRSIN, S. 1951 The decay of isotropic temperature fluctuations in isotropic turbulence. *J. Aero. Sci.* **18**, 417–423.

FINCHAM, A. M., MAXWORTHY, T. & SPEDDING, G. R. 1996 Energy dissipation and vortex structure in freely decaying, stratified grid turbulence. *Dyn. Atmos. Oceans* **23**, 155–169.

FRISCH, U., SHE, Z. S. & THUAL, O. 1986 Viscoelastic behaviour of cellular solutions to the Kuramoto-Sivashinsky model. *J. Fluid Mech.* **168**, 221–240.

GALMICHE, M. & HUNT, J. C. R. 2002 The formation of shear and density layers in stably-stratified turbulent flows: linear processes. *J. Fluid Mech.* **455**, 243–262.

GALMICHE, M., THUAL, O. & BONNETON, P. 1998 Direct numerical simulation of turbulence in a stably stratified fluid and wave-shear interaction. *J. Appl. Sci. Res.* **59**, 111–125.

GALMICHE, M., THUAL, O. & BONNETON, P. 2000 Wave/wave interaction producing horizontal mean flows in stably stratified fluids. *Dyn. Atmos. Oceans* **31**, 193–207.

GARRETT, C. J. R. 1968 On the interaction between internal gravity waves and a shear flow. *J. Fluid Mech.* **34**, 711–720.

GERZ, T. & SCHUMANN, U. 1991 Direct simulation of homogeneous turbulence and gravity waves in sheared and unsheared stratified flows. In *Turbulent Shear Flows 7* (ed. F. Durst, B. E. Launder, W. C. Reynolds, F. W. Schnidt & J. H. Whitelaw), pp. 27–45. Springer.

GERZ, T., SCHUMANN, U. & ELGHOBASHI, S. E. 1989 Direct numerical simulation of stratified homogeneous turbulent shear flows. *J. Fluid Mech.* **200**, 563–594.

GODEFERD, F. S. & CAMBON, C. 1994 Detailed investigation of energy transfers in homogeneous stratified turbulence. *Phys. Fluids* **6**, 2084–2100.

GRIMSHAW, R. 1984 Wave action and wave-mean flow interaction, with application to stratified shear flows. *Annu. Rev. Fluid Mech.* **16**, 11–44.

HANAZAKI, H. & HUNT, J. C. R. 1996 Linear processes in unsteady stably stratified turbulence. *J. Fluid Mech.* **318**, 303–337.

HERRING, J. R. & MÉTAIS, O. 1989 Numerical experiments in forced stratified turbulence. *J. Fluid Mech.* **202**, 97–115.

HOLT, S. E., KOSEFF, J. R. & FERZIGER, J. H. 1992 A numerical study of the evolution and structure of homogeneous stably stratified sheared turbulence. *J. Fluid Mech.* **237**, 499–539.

HOPFINGER, E. J., FLÓR, J. B. & BONNETON, P. 1991 Internal waves generated by a moving sphere and its wake in a stratified fluid. *Exps. Fluids* **11**, 255–261.

HOWARD, N. H. 1961 Note on a paper of John. W. Miles. *J. Fluid Mech.* **10**, 509–512.

HUNT, J. C. R., KAIMAL J. C. & GAYNOR, J. E. 1985 Some observations of turbulence structure in stable layers. *Q. J. R. Met. Soc.* **111**, 793–815.

ITSWEIRE, E. C., HELLAND, K. N. & VAN ATTA, C. W. 1986 The evolution of grid-generated turbulence in a stably stratified fluid. *J. Fluid Mech.* **162**, 299–338.

JACOBITZ, F. G., SARKAR, S. & VAN ATTA, W. 1997 Direct numerical simulations of the turbulence evolution in a uniformly sheared and stably stratified flow. *J. Fluid Mech.* **342**, 231–261.

KIMURA, Y. & HERRING, J. R. 1996 Diffusion in stably stratified turbulence. *J. Fluid Mech.* **328**, 253–269.

KOMORI, S., UEDA, H., OGINO, F. & MIZUSHINA, T. 1983 Turbulence structure in stably stratified open-channel flow. *J. Fluid Mech.* **130**, 13–36.

LELONG, M. P. & RILEY, J. J. 1991 Internal wave-vortical mode interactions in strongly stratified flows. *J. Fluid Mech.* **232**, 1–19.

LESIEUR, M. & SCHERTZER, D. 1978 Amortissement autosimilaire d'une turbulence à grand nombre de Reynolds. *J. de Méc.* **17**, 609–646.

LIENHARD, J. H. & VAN ATTA, C. W. 1990 The decay of turbulence in thermally stratified flow. *J. Fluid Mech.* **210**, 57–112.

LIN, J. T. & PAO, Y. H. 1979 Wakes in stratified fluids. *Annu. Rev. Fluid Mech.* **11**, 317–338.

MAJDA, A. J. & SHEFTER, M. G. 1998 Elementary stratified flows with instability at large Richardson number. *J. Fluid Mech.* **376**, 319–350.

MÉTAIS, O. & HERRING, J. R. 1989 Numerical simulations of freely evolving turbulence in stably stratified fluids. *J. Fluid Mech.* **202** , 117–148.

MILES, J. W. 1961 On the stability of heterogeneous shear flows. *J. Fluid Mech.* **10**, 496–508.

MILLS, R. R., KISTLER, A. L., O'BRIEN, V. & CORRSIN, S. 1958 Turbulence and temperature fluctuations behind a heated grid. *NACA Tech. Note* 4288.

MÜLLER, P. 1976 On the diffusion of momentum and mass by internal gravity waves. *J. Fluid Mech.* **77**, 4, 789–823.

ORSZAG, S. A. & PATTERSON, G. S. 1972 Numerical simulation of turbulence. In *Statistical Models and Turbulence* (ed. M. Rosenblatt & C. Van Atta). Lecture Notes in Physics, Vol. 12, pp. 127–147. Springer.

PARK, Y.-G., WHITEHEAD, J. A. & GNANADESKIAN, A. 1994 Turbulent mixing in stratified fluids: layer formation and energetics. *J. Fluid Mech.* **279**, 279–311.

PEARSON, H. J. & LINDEN, P. F. 1983 The final stage of decay of turbulence in stably stratified fluid. *J. Fluid Mech.* **134**, 195–203.

PHILLIPS, O. M. 1968 The interaction trapping of internal gravity waves *J. Fluid Mech.* **34**, Part 2, 407–416.

PHILLIPS, O. M. 1972 Turbulence in a strongly stratified fluid – is it unstable? *Deep Sea Res.* **19**, 79–81.

PICCIRILLO, P. & VAN ATTA, W. 1997 The evolution of a uniformly sheared thermally stratified turbulent flow. *J. Fluid Mech.* **334**, 61–86.

POSMENTIER, E. S. 1977 The generation of salinity finestructure by vertical diffusion. *J. Phys. Oceanogr.* **7**, 298–300.

RILEY, J. J. & LELONG, M. P. 2000 Fluid motions in the presence of strong stable stratification. *Annu. Rev. Fluid. Mech.* **32**, 613–657.

RILEY, J. J., METCALFE, R. W. & WEISSMAN, M. A. 1981 Direct numerical simulations of homogeneous turbulence in density stratified fluids. *Proc. AIP Conf. on Nonlinear Properties of Internal Waves* (ed. B. J. West), Vol. 76, pp. 79–112.

SPEDDING, G. R. 1997 The evolution of initially turbulent bluff-body wakes at high internal Froude number. *J. Fluid Mech.* **337**, 283–301.

STAQUET, C. & RILEY, J. J. 1989 On the velocity field associated with potential vorticity. *Dyn. Atmos. Oceans* **14**, 93–123.

THUAL, O. 1992 Zero-Prandtl-number convection. *J. Fluid Mech.* **240**, 229–258.

TOWNSEND, A. A. 1976 *The Structure of Turbulent Shear Flow*. Cambridge University Press.

WINTERS, K. B. & D'ASARO, E. A. 1994 Three-dimensional wave instability near a critical level. *J. Fluid Mech.* **272**, 255–284.

YOON, K. & WARHAFT, Z. 1990 The evolution of grid-generated turbulence under conditions of stable thermal stratification. *J. Fluid Mech.* **215**, 601–638.